

Foraminiferal record of Holocene paleo-earthquakes on the subsiding south-western Poverty Bay coastline, New Zealand

Bruce W Hayward, Ashwaq T Sabaa, Hugh R Grenfell, Ursula A Cochran, Kate J Clark, Nicola J Litchfield, Laura Wallace, Mike Marden & Alan S Palmer

To cite this article: Bruce W Hayward, Ashwaq T Sabaa, Hugh R Grenfell, Ursula A Cochran, Kate J Clark, Nicola J Litchfield, Laura Wallace, Mike Marden & Alan S Palmer (2015) Foraminiferal record of Holocene paleo-earthquakes on the subsiding south-western Poverty Bay coastline, New Zealand, *New Zealand Journal of Geology and Geophysics*, 58:2, 104-122, DOI: [10.1080/00288306.2014.992354](https://doi.org/10.1080/00288306.2014.992354)

To link to this article: <https://doi.org/10.1080/00288306.2014.992354>

 [View supplementary material](#)

 Published online: 02 Apr 2015.

 [Submit your article to this journal](#)

 Article views: 447

 [View related articles](#)

 [View Crossmark data](#)

 Citing articles: 5 [View citing articles](#)

RESEARCH ARTICLE

Foraminiferal record of Holocene paleo-earthquakes on the subsiding south-western Poverty Bay coastline, New Zealand

Bruce W Hayward^{a*}, Ashwaq T Sabaa^a, Hugh R Grenfell^a, Ursula A Cochran^b, Kate J Clark^b, Nicola J Litchfield^b, Laura Wallace^c, Mike Marden^d and Alan S Palmer^e

^aGeomarine Research, Remuera, Auckland, New Zealand; ^bGNS Science, Lower Hutt, New Zealand; ^cInstitute of Geophysics, University of Texas, Austin, TX, USA; ^dLandcare Research, Gisborne, New Zealand; ^eInstitute of Natural Resources, Massey University, Palmerston North, New Zealand

(Received 29 July 2014; accepted 24 November 2014)

Foraminiferal faunas in 29 short cores (maximum depth 7 m) of estuarine and coastal wetland sediment were used to reconstruct the middle–late Holocene (last 7 ka) elevational history on the southern shores of Poverty Bay, North Island, New Zealand. This coast is on the southwest side of a rapidly subsiding area beneath western Poverty Bay. Modern Analogue Technique paleo-elevation estimates based on fossil foraminiferal faunas indicate that the four study areas have gradual late Holocene (<3.5 ka) subsidence rates that increase from the southwest (mean c. 0.5 m ka⁻¹) to northeast (mean c. 1.0 m ka⁻¹). Only two rapid, possibly co-seismic, vertical displacement events are recognised: (1) c. 1.2 m of subsidence at 5.7 ± 0.4 ka (cal yr BP), which may have been generated by a subduction interface earthquake centred offshore and recorded in other published studies in northern Hawkes Bay, c. 35 km to the south; and (2) c. 1 m of uplift (relative sea-level fall) at c. 4.5 ± 0.3 ka, which might have been generated by rupture on an offshore upper plate fault that also uplifted coastal terraces at Pakarae and Mahia, 40 km to the north and south of the study area, or by rupture on the subduction interface penetrating beneath Poverty Bay. No sudden displacement events are recognised during the last 4 ka although subsidence, possibly aseismic, has continued.

Keywords: earthquake history; Holocene; intertidal and salt marsh foraminifera; New Zealand; Poverty Bay; sea-level estimates; tectonic subsidence

Introduction

New Zealand lies on the boundary (Hikurangi Margin) between the Pacific and Australian plates with the west-dipping subduction interface passing at relatively shallow depth beneath the east coast of the North Island and Cook Strait (Fig. 1; Williams et al. 2013). Ruptures along similar plate-boundary megathrusts in other places produce the world's largest known earthquakes ($M_w > 9$) and tsunamis (e.g. 1960 Chilean, 1964 Alaska, 2004 Sumatra–Andaman, 2011 Tohoku earthquakes). New Zealand, however, has no historical record of any such large earthquakes ($>M_w 7.2$) since the beginning of historical records (c. 1840 AD) (Eiby 1989; Wallace et al. 2009). The major outstanding question in New Zealand paleoseismology is therefore whether the east coast of the North Island has had periodic megathrust earthquakes during the Holocene and so is likely to experience another sometime in the future. The largest and most damaging

earthquakes in historic times in this region have in most cases been attributed to movement on upper plate faults (e.g. Hull 1990; Doser & Webb 2003; Litchfield et al. 2014).

Using the geological record to distinguish between paleo-earthquakes generated along upper plate faults and those generated on the subduction megathrust is not easy. Due to the length of typical structures in the forearc of the Hikurangi margin, ruptures on upper-plate faults are expected to produce displacements only over relatively localised areas (<50–100 km) (Barnes et al. 2010; Berryman et al. 2011). The vertical component of these displacements is predominantly uplift with only minor local subsidence (e.g. Hull 1990; Berryman 1993a). Typically, megathrust ruptures affect much larger areas (along 500–1500 km of strike) and produce areas of uplift above the source, and subsidence down-dip of the main rupture area (Plafker 1969; Meltzner et al. 2006; Vigny et al. 2011). Conceptually, the evidence for megathrust earthquakes may be complicated, as

*Corresponding author. Email: b.hayward@geomarine.org.nz

Supplementary data available online at www.tandfonline.com/10.1080/00288306.2014.992354

Supplementary file 1: Table S1. Foraminiferal sample data from Holocene sediment cores, coastal south-western Poverty Bay, including raw census counts, relative abundances, absolute densities and MAT paleo-elevation estimates and ranges; **Supplementary file 2:** Table S2. Relative abundances of foraminiferal species in 1016 modern analogue faunal samples from around the coast of New Zealand (including 594 intertidal samples from harbours, estuaries and salt marshes), with tidal elevations used for MAT elevation estimates; **Supplementary file 3:** Table S3. Workbooks showing the construction of land elevation records (LER) (Fig. 7) for a selection of the better-dated Poverty Bay cores; **Supplementary file 4:** Table S4. Earthquake age model for southwest Poverty Bay produced using the program OxCal (v. 4.2, Bronk Ramsey 2009); **Supplementary file 5:** Figure S1. Map of New Zealand showing location of study areas where the paralic and inner-shelf modern analogue foraminiferal faunas were sourced for use in the MAT paleo-elevation estimates; **Supplementary file 6:** Figure S2. Generalised Holocene sea-level curve as currently known for New Zealand and used to adjust elevation histories for Poverty Bay cores.

subduction interface ruptures could also trigger associated upper-plate fault movements (Cummins & Kaneda 2000; Wang & Hu 2006; Melnick et al. 2012).

The present study is part of a larger programme to look for evidence of middle–late Holocene subsidence events that might be coeval along a significant portion of the east New Zealand subduction boundary, between Marlborough and East Cape (Fig. 1). However, most of this stretch of coast has stepped sequences of uplifted Holocene coastal and fluvial terraces that document a segmented regime of net tectonic uplift (e.g. Ota et al. 1988; Berryman et al. 1989; Berryman 1993a; Clark et al. 2010). Each regional segment of the coast has had a separate deformation history, with most segments having been uplifted by a sequence of co-seismic events (uplift c. 1–4 m each) at recurrence intervals of 400–2000 years (Berryman et al. 1989, 2011). It is impossible to find a geologic record of subsidence events in these regions where there is net Holocene uplift.

Sections of subsiding coast provide the only opportunities to capture a record of Holocene subsidence events that may have been caused by megathrust earthquakes. In these places there is the opportunity to use microfossil records of paleo-sea-level height in marginal marine sedimentary sequences to identify sudden substantial (>0.5 m) vertical displacement events (e.g. Guibault et al. 1996; Nelson et al. 1996; Hawkes et al. 2005). Along the targeted coastline there are only four areas that appear to have net Holocene subsidence: south-western Poverty Bay, Hawkes Bay, Porangahau and Big Lagoon, Marlborough (Berryman et al. 1989; Hayward, Grenfell et al. 2006; Hayward, Wilson et al. 2010; Hayward, Grenfell et al. 2012b). The northernmost of these, south-western Poverty Bay (Fig. 1), is the subject of this report where we use microfossil foraminifera in coastal wetland cores to track the Holocene elevational history of the area in an attempt to identify sudden, potentially co-seismic, vertical displacement events.

Aim of this study

The aim of this study was to use foraminiferal-based paleo-elevation estimates from estuarine and lagoonal sediment sequences to determine the middle–late Holocene (last 7 ka) elevational history of south-western Poverty Bay as a contribution to understanding future earthquake risk. It is part of a larger project to try to determine if the east coast of the North Island of New Zealand has a pre-human history of megathrust earthquakes.

Tectonic setting

Poverty Bay lies within the generally uplifted inner forearc portion of the northern Hikurangi Subduction Margin, where the Pacific Plate is being subducted beneath the eastern North Island at rates of c. 20 mm a⁻¹ at southern Hikurangi, increasing to 60 mm a⁻¹ at northern Hikurangi (Wallace et al. 2004). The megathrust subduction interface is c. 15 km beneath our study area (Williams et al. 2013). Offshore, between the coast and the plate boundary, the submerged outer forearc is deformed by reverse faults and associated folds (Fig. 1) (Gerber et al. 2010; Mountjoy & Barnes 2011). Rapid uplift of the inland ranges to

the west (Litchfield & Berryman 2006; Wilson et al. 2007) is thought to be the result of deep-seated subduction processes, including sediment underplating (e.g. Walcott 1987; Litchfield et al. 2007). In places other than our study area, the coastal fringe is being pushed up by slip on offshore thrust faults such as the Lachlan Fault and Gable End Fault (Fig. 1) (Berryman 1993a,b; Wilson et al. 2006; Litchfield et al. 2014). The continental shelf offshore of Poverty Bay comprises two actively uplifting fault-crest anticlines (Lachlan and Ariel) forming the shelf edge separated from the coastline by subsiding sub-basins (Fig. 1) (Gerber et al. 2010).

Water borehole stratigraphy and Holocene radiocarbon dates have been used to divide the Poverty Bay coastal plain into a north-eastern uplift area, a central pivotal area and a south-western subsidence area (Brown 1995) which, with additional borehole data, has been interpreted as southwest tilting during the Holocene beneath the Poverty Bay coastal plain (Berryman et al. 2000; Wolinsky et al. 2010). Our study area is located along the southwest side of this broad area of subsidence (Fig. 1).

A variety of processes may be occurring to generate the contrasting uplift and subsidence observed along the coastline at the northern Hikurangi subduction margin including seamount subduction, deep sediment underplating and Hikurangi Plateau subduction, among others (Litchfield et al. 2007). One possibility for the subsidence in our study area is that it is related to forearc basin development processes, while the contrasting uplift to the northeast and southwest along the margin is a consequence of splay faulting, seamount subduction or subducted sediment underplating (or some combination of these factors). The causes of forearc basin subsidence are not completely clear, and may be due to factors such as isostatic effects from subduction of dense oceanic lithosphere, or thermal cooling of the forearc due to subduction of a colder plate (e.g. Stuwe 2007). It may also be that the subsidence is simply related to the system of anticlines and synclines that have evolved along the east coast margin (e.g. Foster & Carter 1997). There are numerous seamounts subducting along the northern Hikurangi margin (e.g. Collot et al. 1996, 2001). Analogue modelling (Dominguez et al. 1998) suggests that subsidence can occur in the wake of a subducting seamount, so this could be a mechanism to produce subsidence in our study area. Likewise, rapid uplift to the north at Pakarua could also be related to an earlier stage of seamount subduction, whereby the seamount is located in front of or directly beneath the rapidly uplifting region. As the subsidence is isolated to the Poverty Bay area (with uplifting regions to the north and south), we prefer the idea that the local uplift patterns are related to seamount subduction. However, without more precise geophysical imaging beneath the Poverty Bay coastline, discussions of mechanisms for coastal uplift and subsidence are speculative at best.

Study sites

This report provides the lithologic, foraminiferal, inferred paleo-environmental and estimated elevational histories from 29 cores

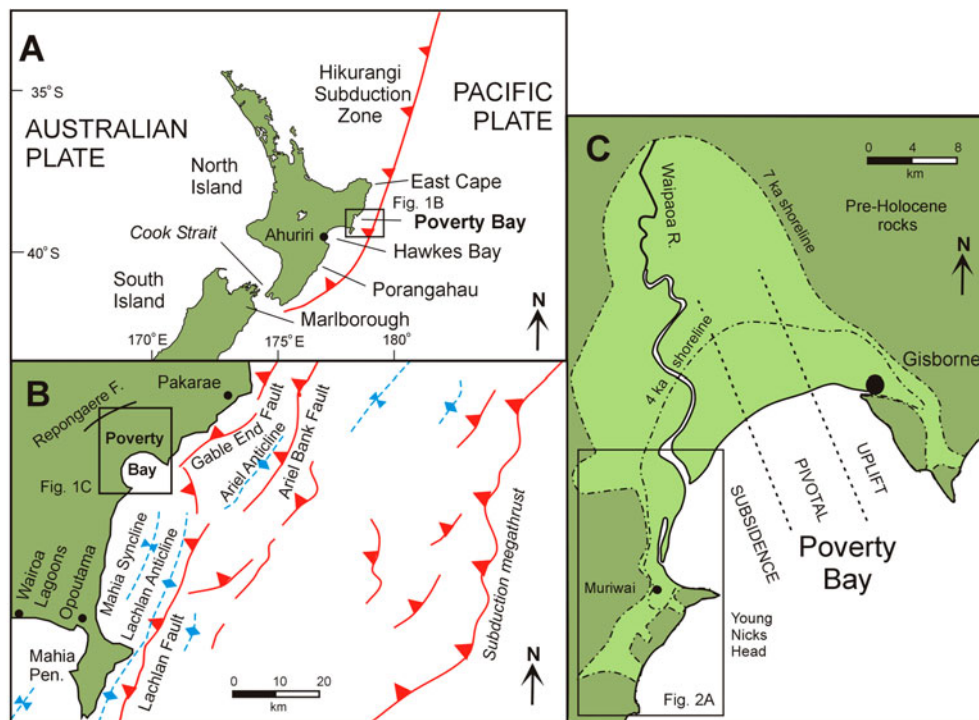


Figure 1 A, Map of Hikurangi subduction margin along the east coast of the North and northern South islands of New Zealand. B, Location of major active faults (solid lines) and folds (dashed lines) in the vicinity of our study area in south-western Poverty Bay (marked rectangular area shown in C). Offshore structure from Lewis et al. (1997), Gerber et al. (2010) and Mountjoy & Barnes (2011). C, Holocene paleoshorelines and tectonic regions of Poverty Bay (after Brown 1995). Rectangle outlines study area shown in Fig. 2A.

taken on four field trips (Fig. 1). Cores were located in the most likely places where Holocene salt marshes may have been present, in order to use the higher-resolution tidal zonation of foraminifera that occurs in this setting for our paleo-elevation studies. The results of initial studies on reconnaissance cores were used to guide subsequent core site selections.

Five cores (Bull 1–5) were taken in Te Hau Valley, a small south-eastern side valley of the Holocene Wherowhero tidal paleo-lagoon (Fig. 2). The western half of the valley is flat-floored and underlain by Holocene sediment. The valley rises gradually and narrows towards the east where it has been beheaded by eroding 20-m-high coastal cliffs. All cores were located on the western valley floor (2.5–3 m above mean sea level, ASL), which has four 0.5–1.5-m-deep drains running NW–SE across it.

Fourteen cores (YN 1–14) were taken in Orongo Valley, a slightly larger side valley of the Wherowhero tidal paleo-lagoon, located c. 1 km northeast of Te Hau Valley (Fig. 2). Orongo is also a flat-floored valley surrounded by steeply sloping hillsides of soft Miocene mudstone (Mazengarb & Speden 2000). Until c. 2010, the low-lying (0.8–2 m ASL) flat-floored valley was swampy pasture and wetland not disturbed for cropping. In the last five years (during the time of coring) the Orongo valley floor has been modified into a series of six freshwater ponds to become a wildlife refuge. The three smallest ponds (Ponds 1–3, Fig. 2C) are in a small north-eastern side valley where the floor slowly rises to 3 m ASL at

the site of core YN 9. The valley floor widens to the northwest where it passes into the coastal terrace around the southern side of present-day Wherowhero Lagoon. The southeast end of the low-lying valley floor is separated from the Pacific Ocean by a sand dune (1.5–3 m ASL) and sandy beach.

Six cores (Mur 1–6) were taken on the low coastal plain along the landward (west) side of the modern Wherowhero Lagoon adjacent to and north of the settlement of Muriwai (Fig. 2D). The lagoon is separated from the open sea by a narrow sand spit and is the abandoned, elongate estuarine mouth of the large Waipāoa River, which currently enters the sea 2.5 km north of our northernmost cores (Mur 1, 4–6). The lagoon is largely intertidal with a meandering tidal channel running its length. Through the Holocene, the Wherowhero Lagoon may have had a varied history, initially much larger and more recently alternating between the estuarine mouth of the large Waipāoa River and a blind lagoon as it is today. The last time it was the river mouth was 1925–1945. In 1946 a groyne was constructed diverting the mouth of Waipāoa River to its present location (Smith 1988). All our Muriwai cores were sited on the coastal plain at elevations close to mean sea level, where foraminiferal faunas in cores indicate that the land level has dropped by c. 0.5–1 m since flood control banks were constructed, a tidal gate installed and drains dug in the 1940s.

Four cores (Tau 1–4) were taken in the Taurau Valley, a wide, flat-floored north-western arm of paleo-Wherowhero Lagoon, 3–4 km west of the mouth of Waipāoa River mouth and 4 km

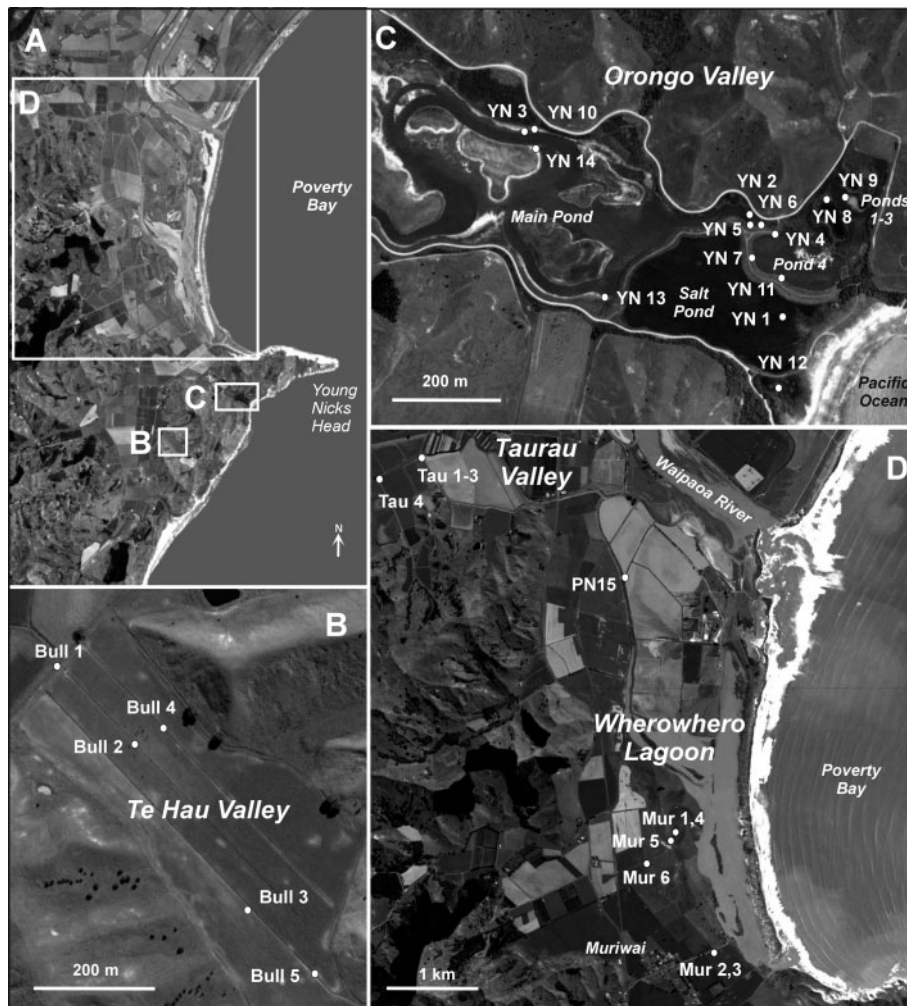


Figure 2 A, Location of Holocene sediment cores in the three study areas on the south-western coast of Poverty Bay (Fig. 1C). B, Te Hau Valley. C, Orongo Valley. D, Muriwai and Taurau Valley.

northwest of cores Mur 1 and 4–6 (Fig. 2D). Here the upper part of the valley floor is filled with alluvial silt and the valley is cut by a 1.5–2.5 m deeply incised stream/drain. All of our cores were acquired in this ditch close to stream water level which, in the case of Tau 1–3, was approximately high tide level (1 m ASL).

Methods

Field sampling

In the field 24 cores were taken in 50 cm lengths using a 3-cm-diameter Eijkelkamp Gouge Auger which is pushed into the ground manually (maximum 4.5 m) and pulled out while rotating the barrel. The advantages of this coring method are that it is relatively quick, the stratigraphy can be examined and recorded as the core is being taken and the core does not suffer from coring compaction effects. Disadvantages are that it returns relatively small samples and is susceptible to contamination from between cored lengths and from the sides of the

hole. These auger cores were lithologically logged and sampled in the field and the remainder discarded.

Five cores (Mur 1, 2, 3, 5; YN 5) were taken using a vibracorer and 7.5-cm-diameter aluminium downpipe. Advantages of this method are that they retrieve a continuous sediment core, potentially up to 7.5 m long and less susceptible to downhole contamination. Disadvantages include the longer time for coring and recovery, the core is not opened in the field and sediment compaction is common. With vibracoring, the hard surface soil crust was removed by digging and the core started in the bottom of the dug hole. These cores were returned to the laboratory to be cut in half lengthwise, lithologically logged and 20 cm³ samples taken for foraminiferal samples at selected intervals. The amount of compaction was measured in the field and used to correct sample core depths to actual depths.

Prior to our main field work, three sections were lithologically logged by one of us (MM) in the sides of excavations for ponds 1–4. Samples of wood were taken for radiocarbon dating and of tephra for geochemical identification.

Surveying

The location and elevations of most of the cores (Appendix 1) were obtained in 2012 by Neville Palmer, GNS Science, using a Leica Real Time Kinematic (RTK) global positioning system and tied back to Land Information New Zealand (LINZ) spot height markers. These elevations were converted to height above (ASL) or below (BSL) mean sea level (MSL = 1.23 m above Chart Datum). The elevations of subsequent cores (Bull 2–5, Mur 6, YN 10–14) were estimated with reference to surveyed core sites, often using water level in non-flowing streams and drains as a proxy for horizontal. The elevations of Taurau Valley cores (Tau 1–4) were estimated using high tide level in the immediately adjacent stream on the day of coring (related back to high tide level for Gisborne).

Laboratory processing

A total of 162 core samples were washed over a 63 μm sieve and dried. The dry sand and mud fractions were weighed separately. Sand fractions were split and examined with the aim of obtaining 100-plus benthic foraminiferal specimens (which was not always possible), which were identified and counted, but not picked. The density of foraminiferal tests per gram of sediment was calculated. Tests were identified with reference to Hayward, Grenfell et al. (1999) and census counts standardised as percentages of the benthic foraminiferal faunas for analyses (see supplementary file Table S1). Other fossil material was recorded as it was encountered. Foraminiferal faunal facies were identified by their dominant or co-dominant species and used for qualitative interpretations of their paleo-environments and paleo-elevation ranges (Appendix 2).

MAT paleotidal elevational estimates

The paleotidal elevation at which each fossil foraminiferal fauna accumulated was estimated using the modern analogue technique (MAT) described in Hayward, Scott et al. (2004) based on the relative abundance of the benthic species, with counts >37 specimens. A squared chord dissimilarity coefficient was used to determine the five most similar modern foraminiferal faunas to each fossil fauna (in terms of faunal composition) using a dataset of 1016 modern samples from shallow New Zealand waters (<50 m depth) including 695 samples from intertidal depths around harbours and estuaries (see Table S2 and Fig. S1). The resulting estimates of tidal elevation or water depth were computed for each fossil fauna as the mean elevation and standard deviation of the five most similar modern faunas (see Table S1). In these calculations, tidal ranges are standardised and converted to the extreme spring tidal range of Poverty Bay (2.0 m) and elevations given relative to MSL.

Reworked or transported foraminifera

The hills behind south-western Poverty Bay are composed of uplifted, relatively soft, deep-marine, Neogene sedimentary rocks.

Reworked fossil foraminiferal tests from this source can be easily recognised by their recrystallised preservation or as bathyal taxa, and have been excluded from our analyses.

Modern foraminiferal tests from exposed offshore shelf environments that have been transported into the quiet estuarine and lagoonal environments of this study during storm or tsunami events are mostly taxonomically distinct (Hayward, Grenfell et al. 1999) and have also been excluded from our paleo-elevation analyses. A few species (e.g. *Bolivina*, *Haynesina depressula*) can live in both quieter offshore waters and subtidal lagoons and estuaries so have been accepted as probably in situ in this study.

Paleo-elevation adjustments for taphonomic loss and infaunal depth

After death, the tests of foraminifera can be removed from the fossil record by selective oxidation and bacterial degradation of the organic cements of agglutinated forms and dissolution of calcareous forms (e.g. Goldstein & Watkins 1999). These processes are more prevalent in the taphonomically active zone (TAZ) (Berkeley et al. 2007) which may be present in the more oxic, upper 10–20 cm of sediment (Loubere et al. 1993). From our studies it appears that a TAZ is more common in salt marshes and meadows between mean high water neap (MHWN) and mean high water spring (MHWS), and less common on intertidal flats or between MHWS and highest astronomical tide (HAT) (*T. salsa* zone).

Dissolution of calcareous tests results from more acidic groundwater, which usually develops where there is decay of abundant organic matter such as in a salt marsh. The establishment of a salt marsh may therefore result in the dissolution of calcareous tests in the underlying 10–20 cm. Calcareous tests can weather away when the sediment remains exposed to the air for long periods, as when relative sea-level falls.

Salt marsh foraminifera are infaunal with peak numbers living in the upper 5–15 cm of the sediment column but may live in decreasing low numbers down to 20–60 cm (e.g. Ozarko et al. 1997; Saffert & Thomas 1998; Hippensteel et al. 2000; Berkeley et al. 2008; Hayward, Figueira et al. 2014). If the environment is changing as sediment accumulates, the deeper infaunal foraminiferal specimens can mix with a fauna of different composition in the underlying layers. If there has been little/no taphonomic loss, then the small numbers of specimens in the deep infaunal tail will not significantly change the overall faunal composition from the earlier environment. If this earlier fauna has been largely or completely lost by taphonomic processes, then the deep infaunal tail of the younger fauna may be all that is present in the fossil record.

We use low foraminiferal test density (<8 g^{-1} sediment) in our samples as a proxy for severe taphonomic loss that may greatly impact our paleo-elevation estimates. MAT estimates based on low density foraminiferal faunas are deemed suspect and possibly the deep infaunal tails of faunas that lived >15 cm above. These suspect faunas are labelled in the paleo-elevation curves.

Calculating the land elevation records

The land elevation records (LER) is a way of graphically portraying (on a time–depth plot) and calculating land elevation changes that might have been caused by seismic or aseismic vertical land displacements. LER have been constructed for each core using the paleo-elevations of well-dated key sample points that were calculated using the following formula (Hayward, Cochran et al. 2004):

$$\text{LER} = D + I + T - H$$

where D is sample depth downcore; I is the indicative tidal elevation (with respect to LAT at the time) at which the sample was deposited (MAT elevation estimate and range of five nearest analogues, based on foraminiferal census counts); T was the paleo-sea level at the time (with respect to present LAT), based on the most recent New Zealand Holocene sea-level curve (see Fig. S2); and H is the elevation of the core at the surface (with respect to present LAT). Key sample points are those that are well dated and have good indicative elevation estimates (I) from the fossil biotas or where sudden changes of I are indicated (see Table S3). No adjustments were made for compaction, as this is treated separately.

Absolute dating

Absolute dates for various levels of some of the cores have been obtained by two methods (Appendix 3):

1. Radiocarbon dating of: unabraded bivalve shells (mostly *Austrovenus stutchburyi*), articulated and in growth position if available; 200–500 calcareous tests of the benthic foraminifer *Ammonia aoteana*; small branches or twigs; or bulk samples of peat or organic-rich mud. Radiocarbon age calibration and earthquake age modelling was undertaken using the program OxCal (v. 4.2, Bronk 2009) and all ages are quoted in calibrated years before present (cal yr BP) with 2-sigma uncertainties (see Table S4).
2. Tephrostratigraphy, using the two common rhyolitic pumice horizons in Poverty Bay. Initial samples were analysed by a JEOL 733 Electron Microprobe. A 10 μm beam diameter and a 8.5 nA beam current were used for all analyses. Most published data for New Zealand tephra cite use of a 20 μm beam but some distal tephra, very vesicular tephra and tuffs are difficult to analyse with a coarsely focused beam. As the 10 μm beam results in high values for Na and slightly lower values for Si than samples on existing databases, the analyst (AP) has re-analysed tephra from type localities and other known sites to construct a new comparative database. At least 10 glass shards were analysed for each sample. Only major oxides and chlorine, which are consistently above the detection limit, were analysed. The two tephra identified by this method were Taupo Tephra (c. 1715 cal yr BP) and Waimihia Tephra (c. 3400 cal yr BP) (Lowe et al. 2013). In later cores the two distinct tephra horizons present in terrestrial, freshwater and salt marsh sequences (not in

intertidal mud flats) were identified by stratigraphic location, macrolithologic differences and correlation (e.g. Pullar 1967).

Results

Summaries of the lithostratigraphy and dominant foraminiferal associations of most cores are presented in Figs 3–5, together with the mean and range of the MAT paleo-elevation estimates based on the faunal census counts. Raw foraminiferal census counts and MAT paleo-elevation estimates are provided in online Table S1.

Inferred paleo-environment histories

Te Hau Valley (cores Bull 1–5)

Below present MSL, all cores consist of slightly carbonaceous, slightly shelly mud which is sandy in the west towards the mouth of this paleo-embayment (Fig. 3). Faunas had moderate to high densities of foraminiferal tests (25–3100 g^{-1} sediment), strongly dominated by *Ammonia* spp. (67–99%) with less common *Elphidium excavatum* (5–32%), indicating accumulation of at least 300 cm of sediment (Bull 4) at sheltered mid–low tidal elevations (MAT estimates 0.1 m ASL to 0.34 m BSL), presumably on the side of a much larger tidal lagoon than the present Wherowhero Lagoon.

Most cores have 70–80 cm of red-brown, laminated, organic-rich soil or peat between the intertidal interval and the base of a 25–70-cm-thick bed of hard white Waimihia Tephra (c. 3400 cal yr BP). This organic-rich sediment lacks foraminifera except for rare tests of intertidal species that we infer may have been transported in by abnormally high king tides. 100–200 cm of clay, soil, peat and thin, coarse Taupo Tephra overlie Waimihia Tephra. We infer that the upper part of the sequences above present MSL accumulated in a terrestrial setting, initially as a shallow coastal plain wetland, becoming dryer in the upper part.

Orongo Valley (cores YN 1–14)

The flat floor of Orongo Valley is underlain by Holocene sediment that was investigated by 14 short cores (Fig. 2C), down to the oldest sediment encountered (YN 3) at c. 5300 cal yr BP (Fig. 4). Between c. 5300 and c. 4500 cal yr BP, much of the valley floor (beneath Main and Salt ponds) accumulated cockle-shell-bearing mud or muddy sand with abundant foraminiferal faunas (50–1350 g^{-1} sediment) dominated by *Ammonia* spp. (75–98%), often with subsidiary *E. excavatum* (up to 15%). The MAT elevational estimates indicate that most of the valley floor was sheltered mid–low tidal flats, presumably as an arm of a much larger ancestral Wherowhero Lagoon. Foraminiferal faunas in the westernmost core (YN3) also contain *Haynesina depressula*, which give low tidal to shallow subtidal paleo-elevation estimates (Fig. 4) and suggest that the arm deepened westwards and was unlikely to have been open to the sea in the east. No cores penetrated right through this shelly unit and the maximum thickness recovered was 150 cm (YN 2, 3). The carbonaceous mud in the lower parts (2.5 m BSL today) of two south-eastern

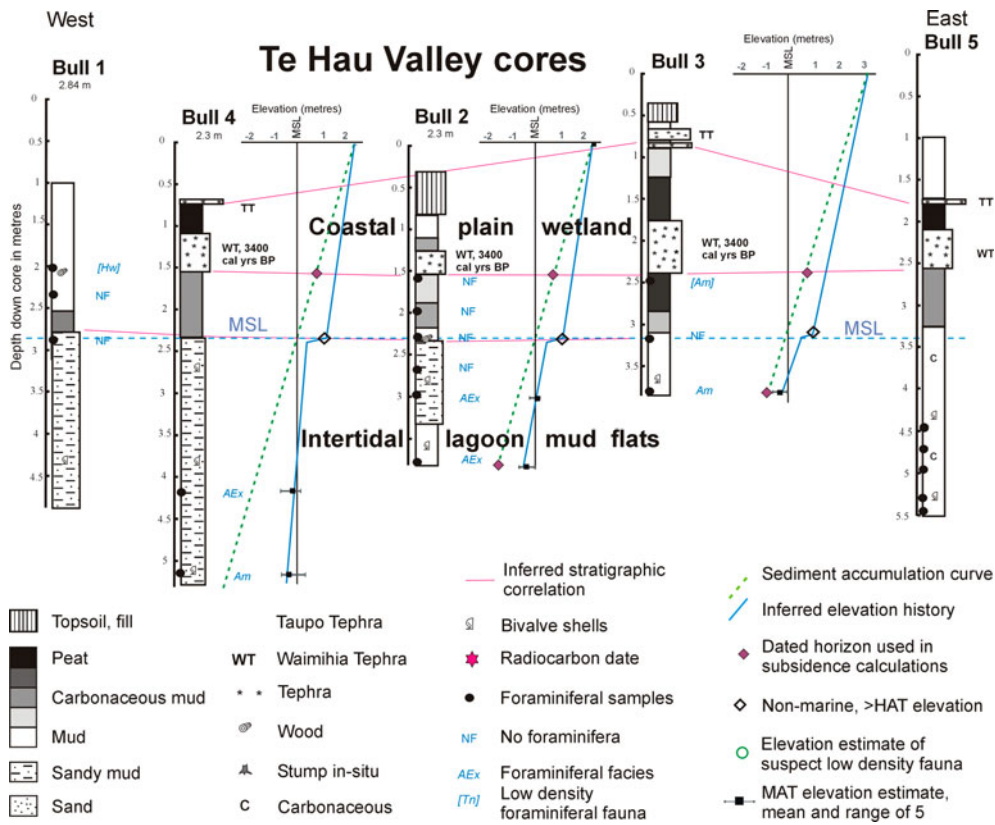


Figure 3 Lithostratigraphy of the Te Hau Valley (Bull) cores (Fig. 2B) aligned with respect to MSL and showing location of foraminiferal samples and their dominant facies composition (Appendix 2). Alongside each core are the plots of MAT elevation estimates (wrt MSL) based on foraminiferal faunas together with ‘error’ bars. Dashed sediment accumulation lines show the downcore elevation of the site if there had been no change in relative sea level during sediment accumulation.

cores (YN 1, 11) contain low-density ($0.2\text{--}0.35\text{ g}^{-1}$ sediment) agglutinated faunas dominated by *Trochammina inflata* that may be all that remain from taphonomically decimated high-salinity, high salt marsh faunas on the edge of the tidal flats.

In many cores (YN 1, 2, 5, 14) the upper 20–100 cm of the shelly mud is unfossiliferous, suggesting that the calcareous *Ammonia* tests have been taphonomically lost, possibly as a result of weathering in contact with air or acidic groundwater associated with the establishment of salt marsh above. Above the shelly unit, almost all cores contain 20–40 cm of carbonaceous or wood-bearing mud, peat or soil directly underlying the 3.4 ka Waimihia Tephra. In the west, a woody mud (YN 3, 175 cm) has a foraminiferal fauna (10 g^{-1} sediment) dominated by the middle marsh species *Haplophragmoides wilberti* (90%) that accumulated near mean high water, MHW level (MAT estimate 0.58 m ASL). There is therefore evidence suggesting that some time before eruption of Waimihia Tephra there was a rapid drop in relative sea level, which could have been caused by tectonic uplift or eustatic sea-level fall. This event has been dated in YN3 at 4500 ± 300 cal yr BP (Fig. 4).

Cores and excavated sections in the floor of the northeast side valley (Ponds 1–3, Fig. 2) contain no evidence for any intertidal sediment. In situ tree stumps (dated at 3850 and 3550

cal yr BP) buried in soil (YN 4, 8) testify to the presence of forest here prior to the Waimihia eruption. These buried stumps are now 1 m BSL (Fig. 4).

Characteristically hard and fine Waimihia Tephra (30–100 cm thick; 3400 cal yr BP) and more coarsely pumiceous Taupo Tephra (5–80 cm thick; 1715 cal yr BP) are identified in most cores and provide good time markers. Their thickness varies considerably, possibly as a result of wash off from the surrounding hills in the decades after deposition. All sequences above the Waimihia Tephra contain no marine or brackish non-vegetated sediment faunas. Many cores do contain evidence of freshwater wetland soils with occasional incursions of displaced salt marsh (*Trochammina salsa*) or sheltered lagoon (*Ammonia*) foraminiferal tests, presumably by storm surges or tsunamis. These suggest that the elevation of the valley floor wetland was close to or just above HAT. The low-density *T. salsa* faunas in YN 10 could be the remains of taphonomically decimated salt marsh faunas that accumulated close to HAT.

Around the fringes of the eastern part of Orongo Valley there are buried in situ tree stumps between the Waimihia and Taupo tephra (YN 4, 9, 12). These must have been growing at elevations above HAT (c. 1.2 m ASL) at the time, but now they lie at 0–0.5 m BSL (Fig. 4).

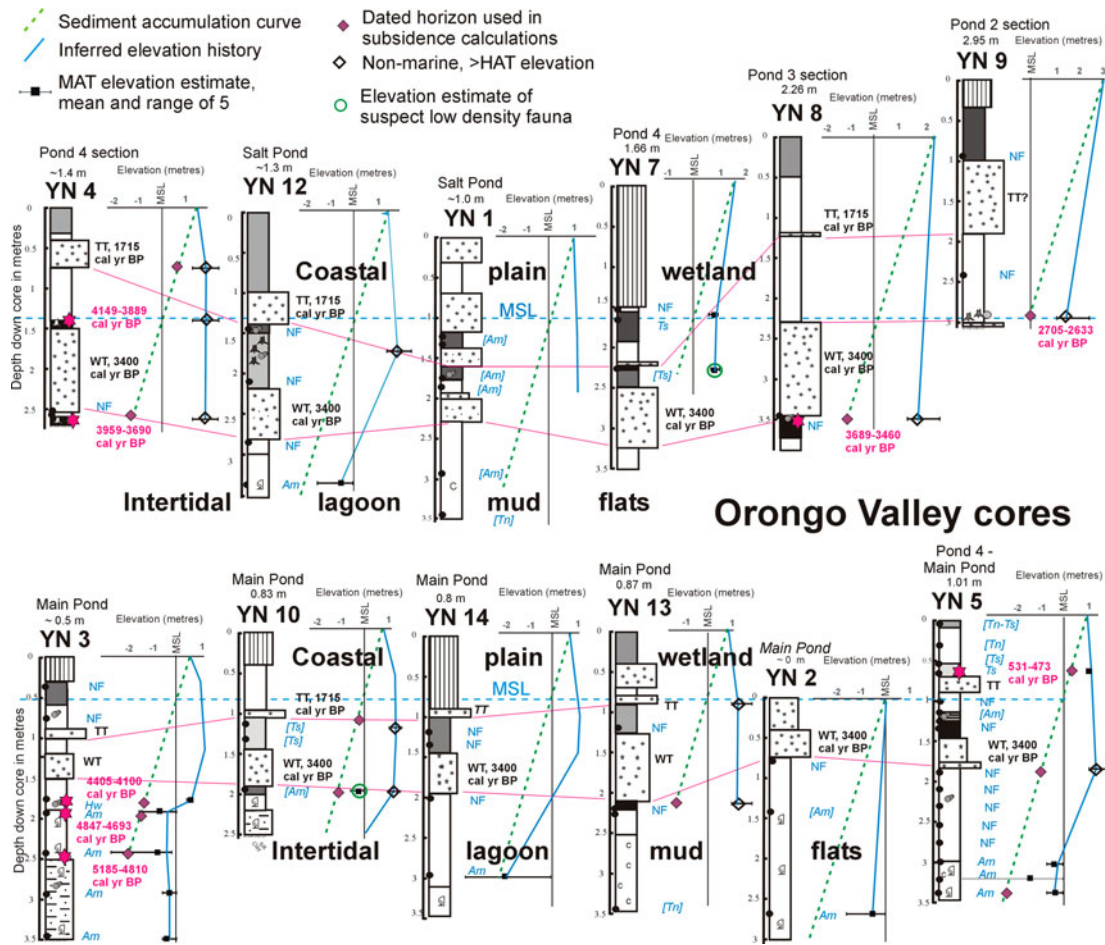


Figure 4 Lithostratigraphy of the 12 more significant Orongo Valley (YN) cores (Fig. 2C) aligned with respect to MSL and showing location of foraminiferal samples and their dominant facies composition (Appendix 2). Alongside each core are the plots of MAT elevation estimates (wrt MSL) based on foraminiferal faunas together with ‘error’ bars. Dashed sediment accumulation lines show the downcore elevation of the site if there had been no change in relative sea level during sediment accumulation. See Fig. 3 for legend.

Two nearby cores (YN 5, 7) in the eastern part of the valley contain moderately low-density ($10\text{--}13\text{ g}^{-1}$ sediment) agglutinated faunas in organic-rich mud between the Taupo Tephra (1715 cal yr BP) and the surface. These faunas are dominated by *T. salsa* (94–100%) and indicate high salt marsh conditions (MAT estimates 0.9–1.05 m ASL) in a brackish lagoon, possibly with periodic incursions of saltwater from the east during storms. Three additional low-density ($0.7\text{--}3\text{ g}^{-1}$ sediment) high salt marsh agglutinated foraminiferal faunas occur in the sediment between Taupo Tephra and the surface in YN 5, suggesting that brackish wetland conditions have covered much of the main part of the Orongo Valley floor for the last 1000 years or so. The elevation of all Main Pond and some Salt Pond cores are today between HAT and MSL and therefore support this hypothesis.

Muriwai, Wherowhero Lagoon cores (cores Mur 1–6)

Six cores were taken from four sites (between MSL and HAT) on the coastal plain along the southern side of Wherowhero Lagoon (Figs 2, 5). The full 7.4 m thickness of the

southernmost cores (Mur 2, 3) consists of shell-bearing mud, fine–medium sand and laminated pumice sand. Foraminiferal faunas ($19\text{--}103\text{ g}^{-1}$ sediment) have a mix of reworked Pliocene (6–65%), transported exposed coast Holocene (1–13%) and sheltered in situ lagoonal species (29–92%). All in situ components are dominated by *Ammonia* spp. (50–87%) with an increasing (shallowing) trend upcore. Subdominants *Elphidium advenum* (6–36%) and *Haynesina depressula* (4–18%) exhibit decreasing upcore trends, consistent with an inferred shallowing from shallow subtidal (AH facies) to low tidal (Am facies) depths. Several well-preserved single valves of the surf clams *Paphies subtriangularis* and *Dosinia anus* from 417 cm were radiocarbon dated at 3923–3625 cal yr BP. All sediment is inferred to have accumulated in the shallow subtidal to low tidal parts of an estuarine lagoon close to its opening to the sea. Reworked Pliocene foraminifera and exposed coast bivalves and foraminifera are inferred to have been swept into the lagoon through its mouth during storms.

The lower 1.5–2 m of the other four Muriwai cores (Mur 1, 4–6) is composed of poorly stratified layers of shell-fragment-

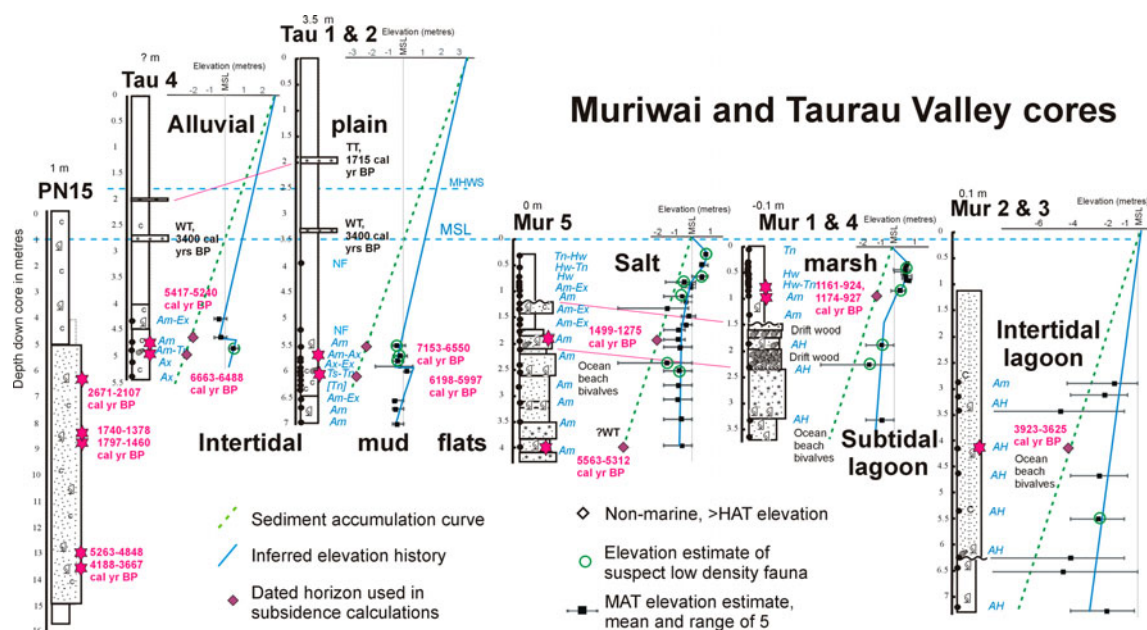


Figure 5 Lithostratigraphy of most of the Muriwai (Mur) and Taurau Valley (Tau) cores (Fig. 2D) aligned with respect to MSL and showing location of foraminiferal samples and their dominant facies composition (Appendix 2). Alongside each core are the plots of MAT elevation estimates (wrt MSL) based on foraminiferal faunas together with ‘error’ bars. Dashed sediment accumulation lines show the downcore elevation of the site if there had been no change in relative sea level during sediment accumulation. Also shown with reduced vertical scale is the stratigraphy of Brown’s (1995) core PN 15 (Fig. 2D). See Fig. 3 for legend.

bearing, dark grey medium–fine sand and grey-white pumiceous coarse sand. Reworked Pliocene tests comprise 15–45% of the foraminifera, transported Holocene tests comprise 9–25% and sheltered lagoonal tests 32–76% with moderate test density (6–21 g^{-1} sediment). The inferred in situ foraminiferal faunas indicate that the sand accumulated in a sheltered estuarine lagoon near its mouth, with the landward core (Mur 5) on low intertidal flats (Am facies) and the seaward cores (Mur 1,4) at spring low tidal to shallow subtidal depths (AH facies). Several thin layers of sheltered estuarine cockle (*A. stutchburyi*) and pipi (*Paphies australis*) are also present. Foraminiferal tests from the deepest cored sand (Mur 5, 396 cm) were dated at c. 5400 cal yr BP (Appendix 3).

The upper 2–2.5 m of cores Mur 1, 4 and 5 consists of driftwood and shelly sand overlain by cockle-shell-bearing mud with the upper 80 cm consisting of organic-rich mud. Foraminiferal faunas (AH facies) suggest that the driftwood beds in Mur 1 and 4 (dated at c. 1350 cal yr BP) accumulated in a quiet low tidal to subtidal backwater pond, possibly behind a sand bar. The overlying shell-bearing mud (double cockles dated at c. 1050 cal yr BP) in all three cores have foraminiferal faunas (5–85 g^{-1} sediment) dominated by *Ammonia*, sometimes with subdominant *E. excavatum* (Am, Am–Ex facies), indicating mid–low tidal depths (MAT estimates 0–1 m BSL). The organic-rich mud has foraminiferal faunas of variable density (0.4–66 g^{-1} sediment) dominated by the agglutinated, high tidal, salt marsh species *Trochammia inflata* and *Haplophragmoides wilberti* (MAT estimates 0.6–0.8 m ASL).

The switch from sand to mud sediment is inferred to be a result of the creation of a quiet tidal backwater with a sand bar separating this area from the main estuarine lagoon to the east. It is likely that the onset of the salt marsh sequence was caused by the rapid eustatic sea-level fall at c. 600 yr BP and the marsh sediment built up as sea level rose c. 0.6 m since then (see Fig. S2). The present elevation of these cores is anomalously low (c. MSL) and is inferred to be a result of drying out and compaction of surface sediment since a stop bank and drain were constructed between the core sites and the estuary in c. 1946, when the Waipāoa River was diverted away from the Wherowhero Lagoon.

Taurau Valley (cores Tau 1–4)

Three cores (Tau 1–3) were located within 10 m of each other in the incised bed of the Taurau Stream beneath a road bridge and the fourth (Tau 4) was 700 m upstream (Fig. 2). The full 700 cm thickness in Tau 1–3 and 550 cm thickness in Tau 4 was mud, except for two 5–10-cm-thick white pumice tephra horizons (Taupo and Waimihia Tephra) at each site. The upper 150–250 cm of mud was weathered and clay-rich, inferred to be coastal plain alluvium. The mud became fresher below MHWS level (Fig. 5), often with carbonaceous specks and cockle shells and fragments (below 1.5 m BSL). The deepest mud (Tau 2, 650–700 cm) contained shell fragments and foraminiferal faunas (48–430 g^{-1} sediment; Am facies) indicating mid–low tidal elevations (MAT estimates of 0.4–0.5 m BSL). This marine mud passed up into a 30–50-cm-thick woody organic-rich mud

(dated at c. 6570 cal yr BP in Tau 4 and c. 6100 cal yr BP in Tau 1) that have no foraminifera or sparse agglutinated or mixed calcareous and agglutinated foraminifera faunas (0.4–52 g⁻¹ sediment; Ax, Ax–Em, Ts–Tn, Am–Tn facies) indicative of salt marsh accumulation at high tidal levels (MAT estimates 0.6–1 m ASL). Above the organic-rich layer there is a sharp transition in the eastern cores (Tau 1–3) back to grey, shell-fragment-bearing mud. In the western core (Tau 4) there is a more gradational transition through carbonaceous mud and a 40 cm woody shell bed (c. 5250 cal yr BP) to grey shell-bearing mud. Foraminiferal faunas from above the organic-rich unit in all cores (1.5–330 g⁻¹ sediment; Am, Am–Ex facies) indicate accumulation on mid–low tidal mud flats (MAT estimates 0.2–0.6 m BSL). The highest cockle shell fragments and foraminifera occur at c. 1.5 m BSL and are inferred to indicate a switch just above them to a terrestrial environment prior to the eruption of Waimihia Tephra at c. 3400 cal yr BP.

Elevational history

In this section we have calculated the amount of subsidence at well-dated depths in the various cores, using the nearest reliable MAT elevational estimates for the mean and the range of the five closest modern analogues. Where in situ tree stumps are present we have estimated the elevation to be at least 1.2 m ASL, and where rare foraminifera are present in otherwise freshwater sediment we have estimated the elevation to be just above HAT (c. 1.2 m ASL). In Table 1, the amounts of subsidence and subsidence rates are given before and after adjustments have been made for the New Zealand Holocene sea-level curve (Fig. S2).

Te Hau Valley

There is no radiocarbon dating control on these cores, but we are confident about the identification of the fine Waimihia Tephra bed (c. 3400 cal yr BP) in Bull 2–5 and Taupo Tephra (1715 cal yr BP) in Bull 3–5. The shell-bearing mud in the lower part of each core accumulated intertidally at around mid-tide level with the oldest (in Bull 4) located c. 3 m BSL today (Fig. 3). Assuming this oldest sediment accumulated between 5000 and 7000 years ago when sea level was c. 1–2 m higher, we get a subsidence of 4.5–5.5 m since then (c. 0.6–1.1 m ka⁻¹ subsidence rate) but less than this if we assume some compaction occurred beneath the base of Bull 4.

The sharp transition from intertidal shell-bearing sediment to terrestrial organic-rich sediment in all cores (c. MSL today) suggests that there was a rapid relative fall in sea level (c. 0.5–1.0 m) sometime prior to Waimihia Tephra (0.75 m below base). This may have been eustatic sea-level fall or tectonically related uplift, which resulted in the establishment of low-lying freshwater wetlands with more acidic groundwater which probably dissolved the original calcareous foraminifera in the now unfossiliferous upper parts of the intertidal mud beneath (Fig. 3).

From the base of the organic-rich sediment upwards it would seem that Te Hau Valley was above HAT, although

perhaps initially not by too much as rare Holocene foraminiferal tests were occasionally washed in (Fig. 3). The base of the Waimihia Tephra is c. 0.75 m above present MSL in Bull 2–5, and is inferred to have been deposited close to HAT (c. 1.2–1.5 m ASL). Since the time of Waimihia eruption, there has therefore been c. 1.35–2.55 m subsidence (eustatic-sea-level corrected) giving a subsidence rate of c. 0.4–0.75 m a⁻¹ during the last 3400 years (Table 1). As the sediment beneath the Waimihia is peat and mud, we assume that a significant amount of this subsidence may be due to compaction.

Orongo Valley

Waimihia and Taupo tephra are recognised in most cores and, together with eight radiocarbon dates, provide the age control for subsidence rate calculations. In all cores the elevation history curves are generally steeper than the sedimentation curves (Fig. 4), indicating increasing relative sea level or subsidence through the studied interval in Orongo Valley. In YN 3, 5, 10, 12 and 14 (Fig. 4) there is an interval prior to eruption of Waimihia Tephra where the elevation history curves are less steep than the sedimentation curves as the sections pass from shell-bearing intertidal sediment up into high tidal (Hw facies) or non-marine peat. As in Te Hau Valley, this may have been a result of rapid eustatic sea-level fall or co-seismic uplift of c. 0.5–1 m. Several cores, particularly YN 3 at 1.8 m BSL, have rather abrupt lithologic or foraminiferal faunal changes that suggest a possible co-seismic subsidence event at about 4500 cal yr BP.

In the westernmost core, YN3, we use dated twigs and the high tidal Hw fauna in peat just below Waimihia Tephra to calculate a eustatic-sea-level-corrected subsidence rate of 0.7–1.0 m ka⁻¹ for the last 4500 years, since the inferred uplift (Table 1, Fig. 6). Further east we have estimated the age of the cockle-bearing mud near the base of core YN5 at 4000–5500 years and derived eustatic-sea-level-corrected subsidence rates of 0.5–1.1 m ka⁻¹ since then and 0.8–1.4 m ka⁻¹ since c. 3400 cal yr ago. The lower rate for the longer time period reflects the possible uplift event c. 3500–4000 cal yr ago.

Three cores/exposed sections in the north-eastern arm of Orongo Valley (YN 4, 8, 9; Fig. 2) are inferred to consist of entirely terrestrial deposits with horizons of in situ tree stumps. These dated forests must have been growing just above HAT at inferred elevations of 1.2–2.2 m ASL when eustatic sea level was 1–2 m higher (Fig. 6). In YN 9 the stumps are currently at MSL, implying there must have been at least 2.2–4.2 m subsidence in the last c. 2700 years (subsidence rate of c. 0.9–1.6 m ka⁻¹). In YN 8 the wood is currently 1.25 m BSL, so there must have been at least 3.2–5.5 m subsidence in the last c. 3550 years (subsidence rate of c. 0.9–1.6 m ka⁻¹). In YN 4 the lower in situ stumps are currently 1.3 m BSL, so there must have been at least 2.5–3.5 m subsidence in the last c. 3800 years (1.0–1.5 m ka⁻¹).

Subsidence rates based on the estimated depositional elevations at the base of the Waimihia and Taupo tephra have been calculated for two other cores (YN 10 and 13; Table 1, Fig. 6).

Table 1 Summary of subsidence calculations for dated horizons with good paleo-elevation estimates. Amount of subsidence = the present elevation of the sample (BSL) less the elevation at which it accumulated (ASL or BSL from MAT or other estimates).

Core	Core depth (m)	Age (cal yr BP)	Present elevation (m)	MAT elevation 5 nearest analogues (m)		Amount of subsidence (m)		Subsidence rates (m ka ⁻¹)	
				Mean	Range	Model 1	Model 2	Model 1	Model 2
Bull 3	2.40	c. 3400	0.75	–	c. 1.2 to 1.5	0.45–0.75	1.35–2.55	0.1–0.2	0.4–0.75
Bull 4	1.55	c. 3400	0.75	–	c. 1.2 to 1.5	0.45–0.75	1.35–2.55	0.1–0.2	0.4–0.75
Mur 1, 4	1.02	1161–924	–1.12	0.10	–0.2 to 0.2	1.0–1.4	1.1–2.5	0.9–1.3	1.0–2.4
Mur 3	4.17	3923–3625	–4.0	–1.8	–4.0 to –0.6	1.2–4.6	2.7–6.6	0.3–1.2	0.7–1.7
Mur 5	1.90	1499–1275	–1.90	–0.77	–1.6 to –0.4	0.8–1.9	0.9–3.0	0.6–1.4	0.7–2.1
Mur 5	3.97	5563–5312	–3.97	–0.57	–1.6 to 0	2.8–4.4	4.1–6.4	0.5–0.8	0.7–1.2
Tau 4	4.70	5460–5130	–2.0	–0.2	–0.6 to 0.1	1.5–2.2	2.7–4.2	0.3–0.4	0.5–0.8
YN 3	1.75	4400–4100	–1.25	0.59	0.44 to 0.65	1.7–1.9	2.9–3.9	0.4–0.5	0.7–1.0
YN 3	1.90	4930–4610	–1.4	–0.71	–1.6 to 0	–0.2–1.4	1.0–3.4	0–0.3	0.2–0.7
YN 3	2.5	5185–4810	–2.0	–0.44	–0.6 to 0	1.4–2.0	2.6–4.0	0.3–0.4	0.5–0.8
YN 4	0.75	c. 1700	0.6	–	c. 1.2 to 2.2	0.6–1.6	0.8–2.8	0.4–0.9	0.5–1.6
YN 4	2.65	3959–3690	–1.3	–	c. 1.2 to 2.2	2.5–3.5	3.3–5.3	0.7–1.0	1.0–1.5
YN 5	0.65	531–473	0.35	1.06	1.0 to 1.1	0.65–0.7	0.0–0.4	1.2–1.5	0.0–0.8
YN 5	1.85	c. 3400	–0.8	–	c. 1.2 to 2.2	2.0–3.0	2.8–4.8	0.6–0.9	0.8–1.4
YN 5	3.36	5500–4000	–2.35	–0.34	–0.62 to 0	1.7–2.3	2.8–4.4	0.3–0.6	0.5–1.1
YN 8	3.5	3689–3460	–1.24	–	c. 1.0 to 2.2	2.4–3.5	3.2–5.5	0.6–1.0	0.9–1.6
YN 9	2.9	2705–2633	0	–	c. 1.2 to 2.2	1.2–2.2	2.5–4.2	0.4–0.9	0.9–1.6
YN 10	1.05	c. 1700	–0.2	–	c. 1.0 to 1.5	1.2–1.7	1.4–2.9	0.6–1.0	0.8–1.7
YN 10	1.9	c. 3400	–1.1	–	c. 1.0 to 1.5	2.1–2.6	2.9–4.4	0.6–0.8	0.8–1.3
YN 13	0.9	c. 1700	–0.05	–	c. 1.0 to 2.0	1.1–2.0	1.3–3.2	0.6–1.2	0.8–1.9
YN 13	2.1	c. 3400	–1.25	–	c. 1.0 to 2.0	2.3–3.3	3.1–5.1	0.7–1.0	0.9–1.5

Model 1 = calculated without any account of eustatic sea-level change; Model 2 = calculated using the New Zealand Holocene sea-level curve (SF Fig. 2).

These give consistent values within the range 0.8–1.5 m ka⁻¹ for the last 3400 years and 0.8–1.9 m ka⁻¹ for the last 1700 years.

Muriwai, Wherowhero Lagoon cores

Apart from the uppermost interval in cores Mur 1, 4 and 5, the MAT-derived elevation history curves in all Muriwai cores are steeper than the sediment accumulation curves (Fig. 5), indicating that there was increasing relative sea level or subsidence through most of the studied intervals. There are no abrupt lithologic or foraminiferal faunal changes that suggest co-seismic subsidence events.

In Mur 1, 4 and 5, a rapid upcore increase in organic matter and a switch from mid–low tidal Am faunas to Hw and Tn high tidal salt marsh faunas at c. 80 cm could record a co-seismic uplift but we infer it is caused by a rapid eustatic fall in sea level at the start of the Little Ice Age c. 600 years ago, as recorded elsewhere around New Zealand (Figueira 2012; Hayward, Grenfell et al. 2012a). The rapid subsidence at the top of these cores has been caused by compaction of the upper layer of organic-rich sediment due to an induced lowering of groundwater levels following the construction of a stop bank c. 50 years ago. Below the upper 80 cm, the eustatic-sea-level-adjusted amount of subsidence for the radiocarbon-dated horizon in Mur 1 (102 cm) is 1.1–2.5 m, giving a subsidence rate of 1.0–2.4 m ka⁻¹ for the last c. 1050 years (Fig. 6, Table

1). In Mur 5 (190 cm, 397 cm) the eustatic-sea-level-adjusted subsidence rates are consistent at 0.7–2.1 m ka⁻¹ for the last c. 1400 years and 0.7–1.2 m ka⁻¹ for the last c. 5300 years. These sediment cores are essentially sand, having deposited in the outer parts of estuary at the mouth of the Waipāoa River, and there is little evidence to imply that subsidence rates should be corrected for compaction.

In Mur 3 at the south end of Wherowhero Lagoon, all faunas give shallow subtidal MAT elevational estimates which have wide confidence limits; at this elevation foraminiferal zones are not as narrow as they are intertidally. The eustatic-sea-level-adjusted amount of subsidence for the radiocarbon-dated horizon (417 cm) is 2.7–6.6 m, giving a subsidence rate of 0.7–1.7 m ka⁻¹ for the last 3775 years (Fig. 6, Table 1). The lowest 1 m of sediment in Mur 3 is subtidal mud, so the estimated subsidence rate may be too high and may need to be adjusted for some compaction beneath the 6-m-thick sand section.

Taurau Valley

All four cores have similar elevational histories with the highest marine indicators at 2 m BSL in Tau 1–3 and at 1.5 m BSL in Tau 4 further to the west (Fig. 5), with inferred non-marine deposition above. All have c. 100 cm of mid–low-tidal shell-bearing mud (MAT estimates 0.2–0.6 m BSL) sharply overlying high-tidal organic-rich sediment (MAT estimates 0.6–1.0 m

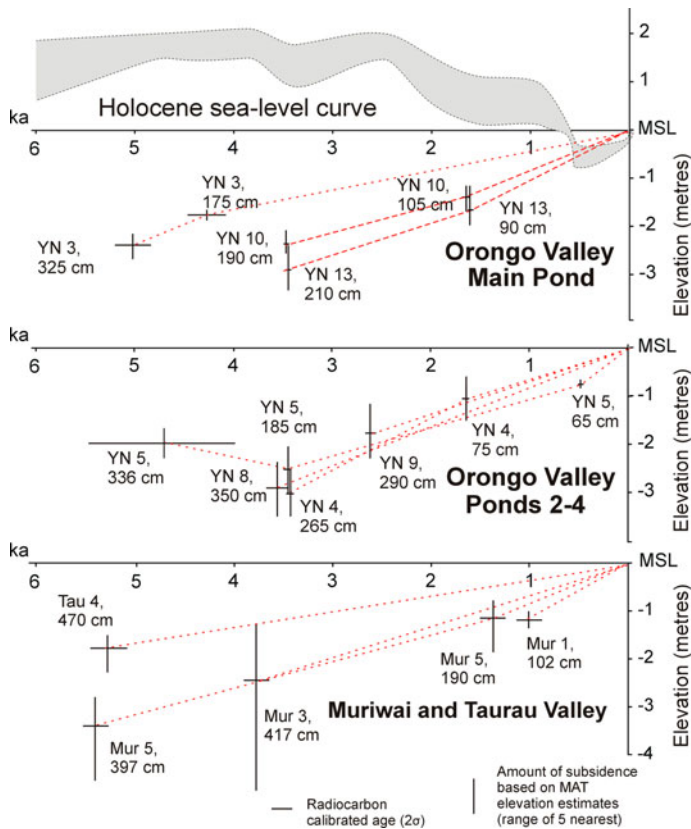


Figure 6 Plots showing the amount of post-depositional subsidence for radiocarbon-dated horizons (Table 1) in cores from Orongo, Muriwai and Taurau valleys, south-western Poverty Bay. These have been calculated using the present-day elevations adjusted for MAT estimated mean and range elevations from the five most similar modern analogue faunas (Fig. 4). The generalised New Zealand Holocene sea-level curve (and accuracy envelope shaded grey) is shown above (see Fig. S2 for sources of data). This allows for eustatic-sea-level-corrected subsidence rates to be calculated (Table 1).

ASL) near the base of the cores. We infer that this widespread contact records 0.8–1.2 m of co-seismic subsidence. The age difference in the two dated samples (6550 and 6100 cal yr BP) could be a result of some post-displacement erosion. Low-tidal *Ammonia* have colonised the upper part of the peat after the inferred seismic event. The age reversal for the overlying dated foraminifera in Tau 2 (c. 6850 cal yr BP) may be due to the small size of the sample and the fact that the *Ammonia* had colonised the older peat. Eustatic-sea-level-corrected amounts of subsidence since the co-seismic subsidence are 2.7–4.2 m, giving a subsidence rate of 0.5–0.8 m ka⁻¹ for the last 6000 years. This rate may be too high as the lower part of the sediment sequence is essentially mud, and no allowance has been calculated for compaction.

Potential co-seismic displacement events

In this study we identify only two possible co-seismic vertical displacement events separating foraminiferal faunas with substantially different MAT elevational estimates. The oldest of

these occurs in all four Taurau Valley cores (Fig. 5), where shell-bearing mud or a shell bed overlies organic-rich sediment or peat at c. 2–2.5 m BSL. MAT elevational estimates suggest a subsidence of 0.8–1.7 m (mean c. 1.2 m) (Fig. 7), although this could have been exaggerated by shaking-induced compaction. Radiocarbon dates bracket this event (Table 1) giving an oxcal (2σ) age of 6097–5299 cal yr BP (Table S4). During this time period three turbidites, inferred to have been earthquake-triggered, have been recorded offshore of Poverty Bay (Pouderoux et al. 2014). This event has not been identified in other south-western Poverty Bay cores in this study because they do not extend this far back in time. This subsidence event could conceivably correlate with a similar subsidence of c. 1 m at c. 5550 cal yr BP recorded in cores 30–40 km to the southwest at Wairoa Lagoons (Cochran et al. 2006). This site is along-strike with south-western Poverty Bay parallel to the subduction interface and offshore Lachlan Fault (Fig. 1). Forward elastic dislocation modelling by Cochran et al. (2006) suggested that c. 1–1.5 m of subsidence at Wairoa Lagoons could be generated by a M_w 7.9–8.1 earthquake rupture on the subduction interface and/or Lachlan Fault, possibly resulting in synchronous uplift of the highest Holocene terrace on Mahia Peninsula (Berryman 1993a) (Fig. 1).

The second vertical displacement is an apparent sharp uplift that is identified in Orongo Valley core YN 3 (Fig. 4). Here at 1.8 m BSL, woody peat with a high tidal salt marsh fauna sharply overlies shell-bearing mud with a low-tidal foraminiferal fauna (Am), indicating a change in relative sea level of 0.6–2.2 m (most probably c. 1 m). Well-preserved broken shells of *Austrovenus* and *Nucula* from 5–15 cm below the contact have been dated at 4848–4696 cal yr BP and woody twigs from peat 0–10 cm above the contact have been dated at 4400–4095 cal yr BP (Appendix 1). The Oxcal (2σ) age of this possible uplift event is 4802–4217 cal yr BP. Comparisons between sediment accumulation curves and elevational history curves suggest that uplift was also recorded around this time in Orongo cores YN5, 10, 12 and 14. This inferred uplift event possibly coincides with the sharp contact between shell-bearing mud overlain by terrestrial organic sediment in the Te Hau Valley cores, 0.6–0.8 m below the base of the Waimihia Tephra (Fig. 3). In offshore Poverty Bay there is one turbidite inferred to have been earthquake-triggered about this time, dated at 4000–4700 cal yr BP (Pouderoux et al. 2014). This uplift event in southwest Poverty Bay could conceivably correlate with that of uplifted terrace T2 (4600–4100 cal yr BP) at Pakarae River mouth (Wilson et al. 2006) 35 km to the north, and the highest terrace (c. 4500 cal yr BP) at Mahia Peninsula (Berryman 1993a) 40 km to the south. Both Pakarae and Mahia terrace sequences have been inferred to be a result of episodic slip on offshore upper plate reverse faults and there is no reason, without improved dating precision, to correlate all three events.

Subsidence rates and compaction

All cores have a record of relative sea-level rise during the middle and/or late Holocene. By comparing our records with

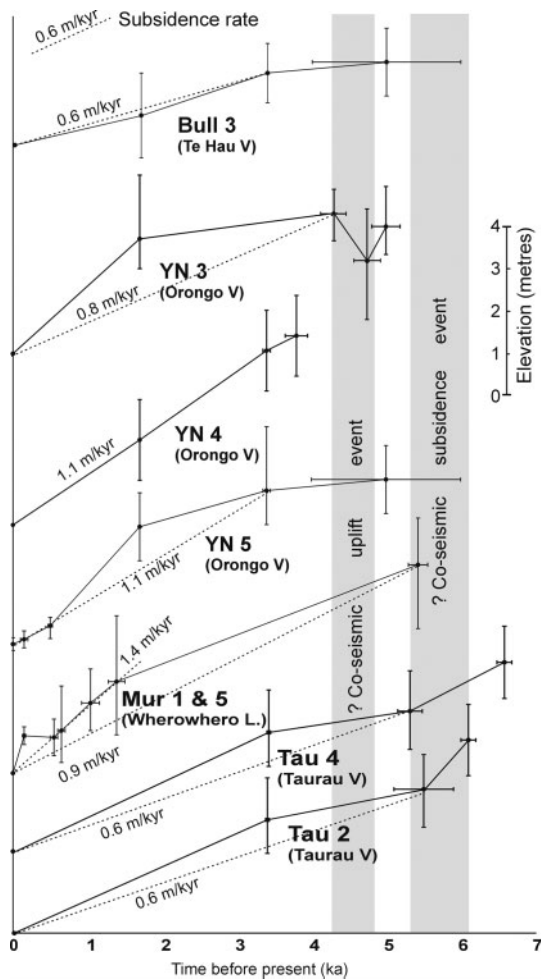


Figure 7 Stacked land elevation record (LER) graphs for a selection of the better-dated cores in south-western Poverty Bay. These show the estimated elevational history of the oldest dated horizon in each core, based on a combination of the sediment accumulation graph, the MAT estimate of depositional elevation and the Holocene eustatic sea-level curve (see Table S3). No adjustments have been made for likely compaction effects. Subsidence rates have been calculated back to the oldest well-dated horizon. Grey shaded bands indicate timing of inferred co-seismic displacement events.

the known New Zealand Holocene sea-level curve (Fig. S2), we infer that all have evidence of subsidence through this period. This subsidence could be tectonic- or compaction-driven (e.g. Allen 1999) or, most likely, a combination of both. There is no good evidence for any sudden subsidence events in the last 5 ka. The subsidence may therefore occur via a continuous, steady process or a combination of numerous small episodic displacements too small to be picked up by the foraminiferal zonation. Calculated subsidence rates for well-dated intervals in the best-studied cores have large uncertainties (Table 1). These wide uncertainties are mostly a result of our imperfect knowledge of New Zealand's Holocene sea-level curve (e.g. Kennedy 2008), which may have been more irregular than currently modelled (especially prior to 1 ka).

Also contributing to these uncertainties are the MAT elevation estimates, especially at elevations below the salt marsh where foraminiferal zones are much broader (e.g. Hayward, Grenfell et al. 2010). In spite of the large uncertainties, the mean subsidence rates for set intervals in cores from the same area show reasonable consistency.

There appears to be a trend of decreasing subsidence from northeast to southwest for the last 3.5–5 ka, with a rate of c. 3 m ka^{-1} in PN 15 (Fig. 2; documented by Brown 1995), to means of c. $0.9\text{--}1.2 \text{ m ka}^{-1}$ in Muriwai cores, c. $0.8\text{--}1.1 \text{ m ka}^{-1}$ in Orongo Valley and c. 0.6 m ka^{-1} in Te Hau Valley and Taurau valleys (Table 1, Fig. 7).

How much of this subsidence can be attributed to compaction of underlying sediment or liquefaction during earthquake-induced shaking is impossible to determine as no cores, except PN 15, penetrated to basement. The amount of compaction will depend on the nature and thickness of the underlying Holocene sediment. Holocene autocompaction ratios of c. 0.2–0.5 have been recorded for estuarine mud and peat with lesser amounts for sand (Bloom 1964; Pizzuto & Schwendt 1997). In all our study locations the cores bottomed in tidal lagoonal mud or muddy sand and this presumably sits directly on fully compacted 'basement', possibly with some fluvial sediment in between. From this we infer that thinner sequences are likely to occur in the side valleys of Te Hau and Orongo than beneath the coastal plain at Muriwai and Taurau. In sites such as Te Hau and Orongo, cores nearer the valley sides are likely to overlie thinner Holocene sequences than near the middle of the valley. The much higher subsidence rate in PN 15 could indeed be partly due to a much greater thickness of Holocene sediment (30 m of fluvial mud; Fig. 3) beneath it. The lower rate for Te Hau Valley could possibly be explained by having a thinner underlying Holocene sequence and therefore less compaction-induced subsidence.

If all or most of the observed subsidence is due to compaction then we might expect far more varying rates of subsidence than observed (Table 1, Fig. 7). Cores were taken from many places in Orongo Valley (Fig. 2) where different thicknesses of underlying compactable sediment would be expected. Using the estimated elevation of the surface onto which the Waimihia Tephra was deposited in the Orongo Valley cores, we can derive an approximation of the amount of subsidence (uncorrected for the eustatic sea-level curve) that has occurred since then (3400 years ago) at each site (Fig. 8). This ranges between 1.7 and 2.7 m. Sites with the least subsidence (<2.2 m) are closest to the foot of the hills on the northern side of the valley (Fig. 8). The largest amount of subsidence (2.7 m in YN 4 and 8) occurs in the north-eastern arm (Fig. 8), where the sediment is dominantly peat or organic-rich mud which compacts more than coarser sediment. This suggests that most of the subsidence >1.7 m may be due to compaction of sediment underlying the Waimihia Tephra in each core. We therefore infer that total tectonically driven subsidence rate in Orongo Valley in the last 3400 years was



Figure 8 Map of Orongo Valley showing the amount of subsidence (in metres) calculated to have occurred at each core site since deposition of Waimihia Tephra, c. 3400 cal yr BP. No eustatic sea-level adjustments (Fig. S2) have been made.

probably no more than 0.8 m ka^{-1} (Fig. 9), when adjusted for higher eustatic sea level.

Unlike Orongo Valley, Te Hau Valley does not extend through to the east coast below sea level. It is therefore unlikely to be as deeply incised and the Holocene sediment fill will be thinner. Cores Bull 2 and 3 record 1.35–2.55 m of subsidence since deposition of Waimihia Tephra, giving a rate of $0.4\text{--}0.75 \text{ m ka}^{-1}$ in the last 3400 years, probably nearer $0.4\text{--}0.5 \text{ m ka}^{-1}$ when corrected for compaction. Taurau Valley was probably similar (Fig. 9).

All cores in the study show evidence of gradual subsidence (Fig. 7). The imprecision of the New Zealand sea-level curve and the likelihood that compaction (either gradual or episodic) contributed to the subsidence means that we are unable to determine whether subsidence rates have been more or less constant throughout the middle-late Holocene or not. The land elevation record graphs (Fig. 7) of some cores (Mur 1, YN 3, 5) suggest faster subsidence since 1.7 ka (Taupo Tephra). This is probably a result of progressive compaction of the cored sequence itself, rather than the contribution from compaction of the sediment beneath the core (i.e. older parts of the cored sequence are likely to have compacted more than younger parts). This internal compaction does not impact the total amount of subsidence of the full cored sequence, only the internal subsidence rates. The inferred sudden uplift event at c. 4500 cal yr BP will also have contributed to the lower net subsidence rates in the interval below the Waimihia Tephra.

Conclusions

In sediment cores from south-western Poverty Bay we have reconstructed Holocene elevation histories using the modern analogue technique (MAT) on fossil foraminifera and conclude the following.

1. Holocene subsidence rates at all sites are greater than that expected from sediment compaction alone and occur gradually.

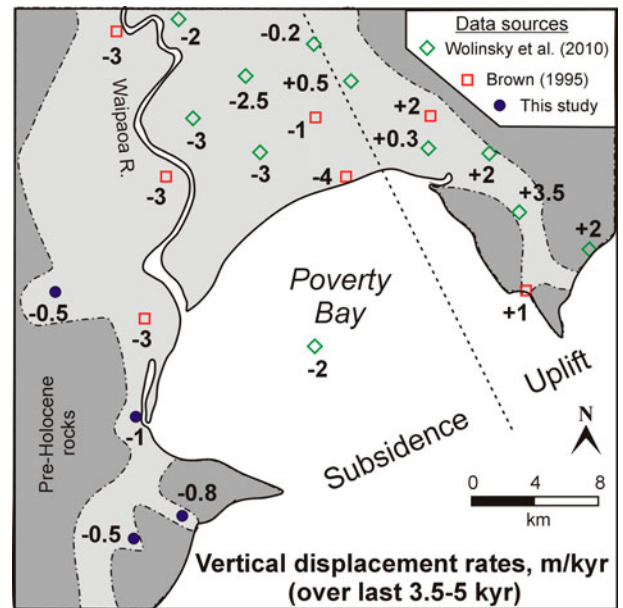


Figure 9 Map of Poverty Bay showing the mean subsidence rates (adjusted for compaction and eustatic sea-level changes) calculated for each of our four study areas over the past 3.5–5 ka. Also shown are the calculated middle-late Holocene rates of subsidence based on dated borehole sequences from central and north-eastern Poverty Bay from Brown (1995), Berryman et al. (2000) and Wolinsky et al. (2010). The offshore Poverty Bay subsidence rate comes from Foster & Carter (1997).

2. A sudden subsidence event at 5700 ± 400 cal yr BP and uplift event at 4500 ± 300 cal yr BP are likely to be earthquake-related involving vertical deformation, and may correlate with similar evidence at other sites along the Hikurangi coastline at similar times.

3. Late Holocene (last 3.5 ka) tectonic subsidence rates increase from southwest (c. 0.5 m ka^{-1}) to northeast (c. 1 m ka^{-1}) through our study area in southern Poverty Bay, with no evidence of any sudden vertical displacements.

Overall we do not see strong evidence for repeated (recurrence times <1.5 ka), large subsidence or uplift events related to subduction interface rupture at this portion of the Hikurangi margin. The subsidence event at 5.7 ± 0.4 ka could represent a large subduction interface earthquake, with the main focus of rupture offshore Poverty Bay. We think it is more likely that the 4.5 ± 0.3 ka uplift event is related to rupture on an offshore upper plate fault, although it could instead be due to rupture on the portion of the subduction interface penetrating beneath the study area. Absence of evidence for repeated subsidence and uplift events in our study area in the last 4 ka does not necessarily mean that subduction thrust events never (or rarely) occur at the northern Hikurangi margin; more work is needed at other coastal sites to confirm this. However, contemporary GPS measurements do suggest that the subduction interface in our study region is currently dominated by steady aseismic creep and slow slip events (Wallace et al. 2004; Wallace & Beavan

2010), and our results are consistent with the possibility that plate motion at this part of the subduction margin has been accommodated largely aseismically for most of the late Holocene.

Acknowledgements

For assistance in the field we thank Jon Kay (2010) and Neville Palmer (2012). Neville is thanked for providing the accurate GPS surveyed location and elevation results for the cores and dune transect. Catherine Reid and Pilar Villamor are thanked for their helpful reviews and editing that have greatly improved the manuscript. For access to their land we thank Ian Foxley (Glendhu Station) and Kim Dodgshun (Nicks Head Station Farm Manager). The Waikato University Radiocarbon Laboratory provided all radiocarbon dates. This research was funded by the Natural Hazards Platform administered by GNS Science.

Supplementary files

Supplementary file 1: Table S1. Foraminiferal sample data from Holocene sediment cores, coastal south-western Poverty Bay, including raw census counts, relative abundances, absolute densities and MAT paleo-elevation estimates and ranges.

Supplementary file 2: Table S2. Relative abundances of foraminiferal species in 1016 modern analogue faunal samples from around the coast of New Zealand (including 594 intertidal samples from harbours, estuaries and salt marshes), with tidal elevations used for MAT elevation estimates.

Supplementary file 3: Table S3. Workbooks showing the construction of land elevation records (LER) (Fig. 7) for a selection of the better-dated Poverty Bay cores.

Supplementary file 4: Table S4. Earthquake age model for southwest Poverty Bay produced using the program OxCal (v. 4.2, Bronk Ramsey 2009).

Supplementary file 5: Figure S1. Map of New Zealand showing location of study areas where the paralic and inner-shelf modern analogue foraminiferal faunas were sourced for use in the MAT paleo-elevation estimates.

Supplementary file 6: Figure S2. Generalised Holocene sea-level curve as currently known for New Zealand and used to adjust elevation histories for Poverty Bay cores.

References

- Allen JRL 1999. Geological impacts on coastal wetland landscapes: some general effects of sediment autocompaction in the Holocene of northwest Europe. *The Holocene* 9: 1–12.
- Barnes PM, Lamarche G, Bialas J, Henrys S, Percher I, Netzeband GL et al. 2010. Tectonic and geological framework of gas hydrates and cold seeps on the Hikurangi subduction margin. *Marine Geology* 272: 26–48.
- Berkeley A, Perry CT, Smithers SG, Horton B 2008. The spatial and vertical distribution of living (stained) benthic foraminifera from a tropical, intertidal environment, north Queensland, Australia. *Marine Micropaleontology* 69: 240–261.
- Berkeley A, Perry CT, Smithers SG, Horton B, Taylor KG 2007. A review of the ecological and taphonomic controls on foraminiferal assemblage development in intertidal environments. *Earth Science Reviews* 83: 205–230.
- Berryman KR 1993a. Age, height, and deformation of Holocene marine terraces at Mahia Peninsula, Hikurangi subduction margin, New Zealand. *Tectonics* 12: 1347–1364.
- Berryman KR 1993b. Distribution, age, height, and deformation of late Pleistocene marine terraces at Mahia Peninsula, Hikurangi subduction margin, New Zealand. *Tectonics* 12: 1365–1379.
- Berryman KR, Marden M, Eden D, Mazengarb C, Ota Y, Moriya I 2000. Tectonic and paleoclimatic significance of Quaternary river terraces of the Waipaoa River, east coast, North Island, New Zealand. *New Zealand Journal of Geology and Geophysics* 43: 225–249.
- Berryman KR, Ota Y, Hull, AG 1989. Holocene paleoseismicity in the fold and thrust belt of the Hikurangi subduction zone, eastern North Island, New Zealand. *Tectonophysics* 163: 185–195.
- Berryman KR, Ota Y, Miyauchi T, Hull AG, Clark K, Ishibashi K et al. 2011. Holocene Paleoseismic history of upper-plate faults in the Southern Hikurangi subduction margin, New Zealand, deduced from marine terrace records. *Bulletin of the Seismological Society of America* 101: 2064–2087.
- Bloom AL 1964. Peat accumulation and compaction in a Connecticut salt marsh. *Journal of Sedimentary Petrology* 34: 599–603.
- Bronk RC 2009. Bayesian analysis of radiocarbon dates. *Radiocarbon* 51: 337–360.
- Brown LJ 1995. Holocene shoreline depositional processes at Poverty Bay, a tectonically active area, northeastern North Island, New Zealand. *Quaternary International* 26: 21–33.
- Clark K, Berryman K, Litchfield N, Cochran U, Little T 2010. Evaluating the coastal deformation mechanisms of the Raukumara Peninsula, northern Hikurangi margin, New Zealand and insights into forearc uplift processes. *New Zealand Journal of Geology and Geophysics* 53: 341–358.
- Cochran U, Berryman K, Zachariasen J, Mildenhall DC, Hayward BW, Southall K et al. 2006. Paleocological insights into subduction zone earthquake occurrence, eastern North Island, New Zealand. *Geological Society of America Bulletin* 118: 1051–1074.
- Collot J-Y, Delteil J, Lewis KB, Davy BW, Lamarche G, Audru J-C et al. 1996. From oblique subduction to intra-continental transpression: structures of the southern Kermadec-Hikurangi margin from multibeam bathymetry, side-scan sonar and seismic reflection. *Marine Geophysical Research* 18: 357–381.
- Collot J-Y, Lewis K, Lamarche G, Lallemand S 2001. The giant Ruatoria debris avalanche on the northern Hikurangi margin, New Zealand: result of oblique seamount subduction. *Journal of Geophysical Research* 106: 19271–19297.
- Cummins PR, Kaneda Y 2000. Possible splay fault slip during the 1946 Nankai earthquake. *Geophysical Research Letters* 27: 2725–2728.
- Dominguez S, Lallemand SE, Malavieille J, von Huene R 1998. Upper plate deformation associated with seamount subduction. *Tectonophysics* 293: 207–224.
- Doser DI, Webb TH 2003. Source parameters of large historical (1917–1961) earthquakes, North Island, New Zealand. *Geophysical Journal International* 152: 795–832.
- Eiby GA 1989. Earthquakes. Revised edition. Auckland, Heinemann Reed. 166 p.
- Foster G, Carter L 1997. Mud sedimentation on the continental shelf at an accretionary margin—Poverty Bay, New Zealand. *New Zealand Journal of Geology and Geophysics* 40: 157–173.

- Gerber TP, Pratson LF, Kuehl S, Walsh JP, Alexander C, Palmer A 2010. The influence of sea level and tectonics on Late Pleistocene through Holocene sediment storage along the high-sediment supply Waipaoa continental shelf. *Marine Geology* 270: 139–159.
- Goldstein ST, Watkins GT 1999. Taphonomy of salt marsh foraminifera: an example from coastal Georgia. *Paleogeography, Palaeoclimatology, Palaeoecology* 149: 103–114.
- Guibault J-P, Clague JJ, Lapointe M 1996. Foraminiferal evidence for the amount of coseismic subsidence during a late Holocene earthquake on Vancouver Island, west coast of Canada. *Quaternary Science Reviews* 15: 913–937.
- Hawkes AD, Scott DB, Lipps JH, Combellick R 2005. Evidence for possible precursor events of megathrust earthquakes on the west coast of North America. *Geological Society of America Bulletin* 117: 996–1008.
- Hayward BW, Cochran UA, Southall K, Wiggins E, Grenfell HR, Sabaa AT 2004. Micropalaeontological evidence for the Holocene earthquake history of the eastern Bay of Plenty, New Zealand. *Quaternary Science Reviews* 23: 1651–1667.
- Hayward BW, Figueira B, Sabaa AT, Buzas MA 2014. Multi-year life spans of high salt marsh agglutinated foraminifera from New Zealand. *Marine Micropaleontology* 109: 54–65.
- Hayward BW, Grenfell HR, Reid CM, Hayward KA 1999. Recent New Zealand shallow-water benthic foraminifera: taxonomy, ecologic distribution, biogeography, and use in paleoenvironmental assessment. *Institute of Geological and Nuclear Sciences Monograph* 21. Lower Hutt, Institute of Geological and Nuclear Sciences. 258 p.
- Hayward BW, Grenfell HR, Sabaa AT 2012a. Marine submersion of an archaic moa-hunter occupational site, Shag River estuary, North Otago. *New Zealand Journal of Geology and Geophysics* 55: 127–136.
- Hayward BW, Grenfell HR, Sabaa AT, Carter R, Cochran U, Lipps JH et al. 2006. Micropaleontological evidence of large earthquakes in the past 7200 years in southern Hawke's Bay, New Zealand. *Quaternary Science Reviews* 25: 1186–1207.
- Hayward BW, Grenfell HR, Sabaa AT, Clark K 2012b. Foraminiferal evidence for Holocene synclinal folding at Porangahau, southern Hawkes Bay, New Zealand. *New Zealand Journal of Geology and Geophysics* 55: 21–35.
- Hayward BW, Grenfell HR, Sabaa AT, Kay J 2010. Using foraminiferal faunas as proxies for low tide level in the estimation of Holocene tectonic subsidence close to the Pacific–Australian plate boundary, New Zealand. *Marine Micropaleontology* 76: 23–36.
- Hayward BW, Scott GH, Grenfell HR, Carter R, Lipps JH 2004. Techniques for estimation of tidal elevation and confinement (~salinity) histories of sheltered harbours and estuaries using benthic foraminifera: examples from New Zealand. *The Holocene* 14: 218–232.
- Hayward BW, Wilson K, Morley MS, Cochran U, Grenfell HR, Sabaa AT et al. 2010. Microfossil record of the Holocene evolution of coastal wetlands in a tectonically–active region of New Zealand. *The Holocene* 20: 405–421.
- Hippensteel SP, Martin RE, Nikitina D, Pizzuto JE 2000. The formation of Holocene marsh foraminiferal assemblages, middle Atlantic coast, USA: implications for Holocene sea level change. *Journal of Foraminiferal Research* 30: 272–293.
- Hull AG 1990. Tectonics of the 1931 Hawke's Bay earthquake. *New Zealand Journal of Geology and Geophysics* 33: 309–322.
- Kennedy DM 2008. Recent and future high sea levels in New Zealand: a review. *New Zealand Geographer* 64: 105–116.
- Lewis KB, Collot J-Y, Davy BW, Delteil J, Lallemand SE, Uruski C et al. 1997. North Hikurangi GeodyNZ swath maps: depths, texture, and geological interpretation. NIWA Chart, Miscellaneous Series 72.
- Litchfield NJ, Berryman KR 2006. Relations between postglacial fluvial incision rates and uplift rates in the North Island, New Zealand. *Journal of Geophysical Research* 111: F02007.
- Litchfield NJ, Ellis S, Berryman K, Nicol A 2007. Insights into subduction–related uplift in the Hikurangi Margin, New Zealand, using numerical modelling. *Journal Geophysical Research* 112: F02021.
- Litchfield NJ, Van Dissen RJ, Sutherland R, Barnes PM, Cox SC, Norris R et al. 2014. A model of active faulting in New Zealand. *New Zealand Journal of Geology and Geophysics* 57: 32–56.
- Loubere P, Gary A, Lagoe M 1993. Generation of the benthic foraminiferal assemblage: theory and preliminary data. *Marine Micropaleontology* 20: 165–181.
- Lowe DJ, Blaauw M, Hogg AG, Newnham RM 2013. Ages of 24 widespread tephras erupted since 30,000 years ago in New Zealand, with re–evaluation of the timing and palaeoclimatic implications of the Lateglacial cool episode recorded at Kaipo bog. *Quaternary Science Reviews* 74: 170–194.
- Mazengarb C, Speden IG 2000. *Geology of the Raukumara area*. Institute of Geological and Nuclear Sciences Map 6. Lower Hutt, Institute of Geological and Nuclear Sciences.
- Melnick D, Moreno M, Motagh M, Cisternas M, Wesson RL 2012. Splay fault slip during the Mw 8.8 2010 Maule Chile earthquake. *Geology* 40: 251–254.
- Meltzner AJ, Sieh K, Abrams M, Agnew CD, Hudnut KW, Avouac J-P et al. 2006. Uplift and subsidence associated with the great Aceh–Andaman earthquake of 2004. *Journal of Geophysical Research* 111: B02407.
- Mountjoy JJ, Barnes PM 2011. Active upper plate thrust faulting in regions of low plate interface coupling, repeated slow slip events, and coastal uplift: example from the Hikurangi Margin, New Zealand. *Geochemistry Geophysics Geosystems* 12: Q01005.
- Nelson AR, Shennan I, Long AJ 1996. Identifying coseismic subsidence in tidal–wetland stratigraphic sequences in the Cascadia subduction zone of western North America. *Journal of Geophysical Research* 101: 6115–6135.
- Ota Y, Berryman KR, Hull AG, Miyauchi T, Iso N 1988. Age and height distribution of Holocene transgressive deposits in eastern North Island, New Zealand. *Paleogeography, Paleoclimatology, Paleoecology* 68: 135–151.
- Ozarko DL, Patterson RT, Williams HFL 1997. Marsh foraminifera from Nanaimo, British Columbia (Canada); implications of infaunal habitat and taphonomic biasing. *Journal of Foraminiferal Research* 27: 51–68.
- Pizzuto JE, Schwendt AE 1997. Mathematical modeling of autocompaction of a Holocene transgressive valley–fill deposit, Wolfe Glade, Delaware. *Geology* 25: 57–60.
- Plafker G 1969. Tectonics of the March 27, 1964, Alaska earthquake. *US Geological Survey Professional Paper* 543-1. Reston, VA, US Geological Survey. 174 p.
- Pouderoux H, Proust J-N, Lamarche G 2014. Submarine paleoseismology of the northern Hikurangi subduction margin of New Zealand as deduced from Turbidite record since 16 ka. *Quaternary Science Reviews* 84: 116–131.
- Pullar WA 1967. Taupo pumice mineralogical anomalies at Gisborne. *New Zealand Science Reviews* 21: 21–22.
- Saffert H, Thomas E 1998. Living foraminifera and total populations in salt marsh peat cores: Kelsey Marsh (Clinton, CT) and the Great Marshes (Barnstable, MA). *Marine Micropaleontology* 33: 175–202.
- Smith RK 1988. Poverty Bay, New Zealand: a case of coastal accretion 1886–1975. *New Zealand Journal of Marine and Freshwater Research* 22: 135–141.
- Stüwe K 2007. *Geodynamics of the Lithosphere*. Berlin, Springer-Verlag. 449 p.

- Vigny C, Socquet A, Peyrat S, Ruegg J-C, Métois M, Madariaga R et al. 2011. The 2010 Mw 8.8 Maule Megathrust earthquake of Central Chile, monitored by GPS. *Science* 332: 1417–1421.
- Walcott RI 1987. Geodetic strain and the deformational history of the North Island of New Zealand during the late Cainozoic. *Philosophical Transactions of the Royal Society of London A321*: 163–181.
- Wallace LM, Beavan J 2010. Diverse slow slip behavior at the Hikurangi subduction margin, New Zealand. *Journal of Geophysical Research* 115: B12402.
- Wallace LM, Beavan J, McCaffrey R, Darby D 2004. Subduction zone coupling and tectonic block rotations in the North Island, New Zealand. *Journal of Geophysical Research* 109: B12406.
- Wallace LM, Reyners M, Cochran U, Bannister S, Barnes P, Berryman K et al. 2009. Characterising the seismogenic zone of a major plate boundary subduction thrust: the Hikurangi Margin, New Zealand. *Geochemistry, Geophysics, Geosystems* 10: Q10006.
- Wang K, Hu Y 2006. Accretionary prisms in subduction earthquake cycles: the theory of dynamic Coulomb wedge. *Journal of Geophysical Research* 111: B06410.
- Williams CA, Eberhart-Phillips D, Bannister S, Barker DHN, Henrys S, Reyners M et al. 2013. Revised interface geometry for the Hikurangi subduction zone, New Zealand. *Seismological Research Letters* 84: 1066–1073.
- Wilson K, Berryman R, Cochran U, Little T 2007. Holocene coastal evolution and uplift mechanisms of the northeastern Raukumara Peninsula, North Island, New Zealand. *Quaternary Science Reviews* 26: 1106–1128.
- Wilson K, Berryman R, Litchfield N, Little T 2006. A revision of mid-late Holocene marine terrace distribution and chronology at the Pakarua River mouth, North Island, New Zealand. *New Zealand Journal of Geology and Geophysics* 49: 477–489.
- Wolinsky MA, Swenson JB, Litchfield N, McNinch JE 2010. Coastal progradation and sediment partitioning in the Holocene Waipaoa Sedimentary System, New Zealand. *Marine Geology* 270: 94–107.

Appendix 1

Table A1.1 Poverty Bay core site locations and depths.

Core	FRF	NZMG Easting	NZMG Northing	Elevation above MSL (m)	Length (m)	Depth cored below surface
Bull 1	Y18/f673	2028219.9	5697158.8	1.69	3.0	4.24
Bull 2	Y18/f674	2028370	5697000	2.3	3.5	3.8
Bull 3	Y18/f675	2028480	5696800	c. 3.2	3.5	3.5
Bull 4	Y18/f676	2028410	5697050	c. 2.3	4.5	5.4
Bull 5		2028560	5696700	c. 3.5	4.5	5.5
Mur 1	Y18/f677	2028461.8	5700563.1	0.1	2.9	4.8
Mur 2	Y18/f678	2028847.4	5699289.9	0.1	2.0	3.4
Mur 3	Y18/f679	2028847.4	5699289.9	0.1	5.7	7.28
Mur 4	Y18/f680	2028457.8	5700559.9	-0.1	1.0	1.0
Mur 5	Y18/f681	2028405.1	5700453.1	-0.1	3.6	4.25
Mur 6		2028080	5700270	c. 0.5	4.5	5.1
Tau 1	Y18/f694	2025930	5704640	3.6	3.5	6.1
Tau 2	Y18/f695	2025930	5704640	3.6	4.5	7.1
Tau 3		2025930	5704640	3.6	4.0	6.6
Tau 4	Y18/f696	2025480	5704390	c. 2.8	4.5	5.5
YN 1	Y18/f682	2030100	5697780	c. 1.0	3.5	3.5
YN 2	Y18/f683	2030050	5698000	c. 0	3.5	3.5
YN 3	Y18/f684	2029620	5698180	c. 0.5	3.5	3.5
YN 4	Y18/f685	2030107.7	5697934.9	c. 1.4	2.7	2.7
YN 5	Y18/f686	2030068.4	5697952.7	1.01	2.9	3.43
YN 6		2030085.8	5697953.3	0.97	3.5	3.5
YN 7	Y18/f687	2030066.5	5697883.5	1.66	3.5	3.5
YN 8	Y18/f688	2030210.2	5697996.5	2.26	3.98	3.98
YN 9	Y18/f689	2030243.8	5697999.6	2.95	3.5	3.5
YN 10	Y18/f690	2029678.2	5698171.4	0.83	2.5	2.5
YN 11		2030140	5697900	1.8	3.5	3.5
YN 12	Y18/f691	2030080	5697660	c. 1.3	3.5	3.5
YN 13	Y18/f692	2029760	5697880	0.87	3.5	3.5
YN 14	Y18/f693	2029630	5698150	0.8	3.5	3.5

FRF, New Zealand Fossil Record file number.

Appendix 2

Table A2.1 Foraminiferal facies abbreviations used in figures and their paleo-environmental meaning.

AH	<i>Ammonia-Haynesina</i>	sheltered subtidal sediment
Am	<i>Ammonia</i> spp.	sheltered low-mid tidal sand/ mud flats
Ax	<i>Ammobaculites exiguus</i>	sheltered low-mid tidal sand/ mud flats
Ax-Ex	<i>A. exiguus-Elphidium excavatum</i>	with dissolution loss of all calcareous tests
Am-Ex	<i>Ammonia-Elphidium excavatum</i>	sheltered low-mid tidal sand/ mud flats
Hw	<i>Haplophragmoides wilberti</i>	salt marsh c. MHWS
Hw-Tn	<i>H. wilberti-Trochammina inflata</i>	salt marsh c. MHWS
NF	No fauna	
Tn	<i>Trochammina inflata</i>	salt marsh between MHWS and HAT
Tn-Ts	<i>T. inflata-Trochammina salsa</i>	salt marsh between MHWS and HAT
Ts	<i>Trochammina salsa</i>	salt marsh c. HAT

Appendix 3

Sample numbers prefixed by Wk are from Waikato University and by NZC from GNS Science radiocarbon laboratories. All dates have been calibrated using Oxcal v.4.2. PN 15 and dates come from Brown (1995) and have been recalibrated for use.

Table A3.1 Radiocarbon ages and tephra identifications from Poverty Bay cores.

Core and depth (cm)	Catalogue No.	Material dated	$\delta^{13}\text{C}$ (‰)	Age (radiocarbon years BP)	Calibrated calendar years BP (confidence)
Mur 1, 70	Wk36224	Lg single, unabraded cockle	-0.6	1480 ± 25	1161–924 (95.4%)
Mur 3, 417	Wk36225	Lg single, unabraded cockle	0.5	3818 ± 27	3923–3625 (95.4%)
Mur4, 85–95	Wk36226	Two sl abraded single cockles	-0.6	1494 ± 26	1174–927 (95.4%)
Mur 5, 190	Wk36227	Double unabraded cockle	-1.0	1820 ± 25	1499–1275 (95.4%)
Mur 5, 395–397	Wk37664	Ammonia foraminifera tests	–	5077 ± 25	5563–5312 (95.4%)
Tau 1, 600–610	Wk37663	Organic-rich sediment	-26.5	5365 ± 20	6198–5997 (95.4%)
Tau 2, 580–590	Wk38748	Ammonia foraminifera tests	–	6364 ± 124	7153–6550 (95.4%)
Tau 4, 465–475	Wk38747	Small unabraded cockles	–	4957 ± 25	5415–5240 (95.4%)
Tau 4, 485–495	Wk38746	Peat	–	5816 ± 28	6663–6488 (95.4%)
YN3, 170–180	Wk39375	Woody twigs	–	3872 ± 25	4405–4100 (95.4%)
YN3, 185–195	Wk39374	Broken cockles and nut shells	–	4569 ± 25	4847–4696 (95.4%)
YN3, 230–270	Wk29687	Double cockles	-0.2	4703 ± 35	5185–4810 (95.4%)
YN5, 55–57	Wk36522	Organic rich sediment	-26.0	486 ± 25	531–473 (95.4%)
YN pond 2 section, 278	Wk17229	Root of in situ tree stump	-26.7	2439 ± 55	2705–2326 (95.4%)
YN pond 3 sect, 328–378	05610	White tephra		Waimihia Tephra	Alan Palmer probe
YN pond 3 sect, c. 390	Wk17019	Wood	-26.8	3393 ± 41	3689–3460 (95.4%)
YN pond 4 sect, 40–45	0561	Coarse tephra		Taupo Tephra	Alan Palmer probe
YN pond 4 sect, 45–48	0562	Tephra		Taupo Tephra	Alan Palmer probe
YN pond 4 sect, 48–50	0563	Tephra		Taupo Tephra	Alan Palmer probe
YN pond 4 sect, 70–75	0564	Hard tephra		Hatepe Lapilli	Alan Palmer probe
YN pond 4 sect, 150	Wk17017	Log	-24.6	3736 ± 40	4149–3889 (95.4%)
YN pond 4 sect, 180–183	0565	Green-white tephra		Waimihia Tephra	Alan Palmer probe
YN pond 4 sect, 210–213	0566	Green-grey fine tephra		Waimihia Tephra	Alan Palmer probe
YN pond 4 sect, 224–225	0567	Cream white tephra		Waimihia Tephra	Alan Palmer probe
YN pond 4 sect, 236–238	0568	Grey-cream fine tephra		Waimihia Tephra	Alan Palmer probe
YN pond 4 sect, 250–253	0569	Cream white tephra		Waimihia Tephra	Alan Palmer probe
YN pond 4 sect, c. 270	Wk17018	Log and in situ stumps	-24.9	3582 ± 40	3959–3690 (95.4%)
PN 15, 650	NZC5303	Shell	–	2652 ± 102	2671–2107 (95.4%)
PN 15, 850	NZC5428	Shell	–	1999 ± 71	1740–1378 (95.4%)
PN 15, 870	NZC5304	Shell	–	2043 ± 64	1797–1460 (95.4%)
PN 15, 1000	NZC6499	Shell	–	4948 ± 40	5436–5135 (95.4%)
PN 15, 1300	NZC5305	Shell	–	4776 ± 77	5263–4848 (95.4%)
PN 15, 1350	NZC5429	Shell	–	3925 ± 98	4188–3667 (95.4%)